Master thesis : Fatigue Methodology of Floating Offshore Wind Turbine Platform & Tower in Composite Materials

Auteur : Pathak, Pharindra
Promoteur(s) : 18532
Faculté : Faculté des Sciences appliquées
Diplôme : Master : ingénieur civil mécanicien, à finalité spécialisée en "Advanced Ship Design"
Année académique : 2021-2022
URI/URL : http://hdl.handle.net/2268.2/16557

Fatigue Methodology for Floating Offshore Wind Power Platform and Turbine Tower in Composite Materials

Submitted on 21st August 2022

By

PATHAK Pharindra | 5-7 Esp. de la Pierre Percée | 44300 Nantes |

Pharindra.Pathak-@eleves.ec-nantes.fr

Student ID No.: 210639D

First Reviewer:

Guillaume DUCROZET

Associate Professor at

Ecole Centrale de Nantes

1, rue de la noë

44321, Nantes

France

Second Reviewer:

Sandrine AUBRUN

Professor at

Ecole Centrale de Nantes

1, rue de la noë

44321, Nantes

France

EMship+ Advanced Design

Abstract

The offshore wind power industry is gaining popularity for generating large amount of electricity around the globe. In recent years, it has developed wind turbine and floater technologies, where abundant wind resources and open sea areas are ideal for developing wind farms. A wind turbine needs a reliable structural design to harvest energy from surrounding environmental loads. However, it is common for offshore wind turbines to be exposed to high dynamic loads, eventually causing fatigue in their substructure.

To overcome the above limitation, a composite material for the wind turbine is a practical alternative. It reduces the maintenance and upkeep costs associated with the steel offshore. It also reduces the tower mass and, the support mass. In this master thesis, methodology for the fatigue assessment of a composite wind turbine tower that can be used on a floating offshore platform has been discussed and finite element models are developed. Additionally, different dynamic analyses and finite element routines are incorporated into the design process of the turbine tower model.

The thesis report has presented the fatigue methodology for the Floating Offshore Wind Power Platform and Turbine Tower in Composite Materials. First, it explains why fatigue life modelling methods for metals and alloys, already developed and validated, cannot be directly applied to composites. Hence, to develop an efficient fatigue model for composite materials, it is imperative to understand the specific mechanisms that cause the damage to a composite material under fatigue and static loading. Next, a particular emphasis has been placed on designing and developing turbine towers using composite materials. The model developed has been run under different load conditions. The repetitive environment load is analysed using BV's in-house software OPERA to evaluate global structural response. At last, the SN curves and CFL diagrams have been used to figure out fatigue life damage using the python script.

Acknowledgment

Bureau Veritas Marine & Offshore has been a unique experience for me during the past six months. My thanks go out to the Composite Materials Section team, namely Mr. PABOEUF Stéphane, Mr. DEYDIER Maxime and Mr. COLLIER Benjamin, for helping me overcome obstacles.

But most importantly, I would like to thank my thesis supervisor, Mr. PETITEAU Jean Christophe, for giving me this opportunity. As a professional, he was the most humane, tolerant, and kind person I have ever met. I will always be grateful to him.

For their help and valuable inputs while learning OPERA and HydroStar, I would be remiss if I did not thank MARTIN Sébastien and BRUN Cedric from the Hydrodynamic department.

I would like to thank every professor I have had for the past two years, both at the University of Liege and at Ecole Centrale de Nantes, and especially professor RIGO Philippe for believing in me and guiding me at every step of my master journey.

I would also like to thank my colleagues, my friends for sharing their thoughts, knowledge and support.

The last, but certainly not the least. I dedicate this to my family. The lighthouse that guides me through an ocean of doubts and fears. It would be impossible for me to conduct this humble work without you, and I dedicate it to you.

France, 21st August 2022
Pharindra Pathak

DECLARATION OF AUTHORSHIP

I declare that this thesis and the work presented in it are my own and have been generated by me as the result of my own original research.

Where I have consulted the published work of others, this is always clearly attributed.

Where I have quoted from the work of others, the source is always given. Apart from such quotations, this thesis is entirely my own work.

I have acknowledged all main sources of help.

Where the thesis is based on work done by myself jointly with others, I have made clear exactly what was done by others and what I have contributed myself.

This thesis has no material that has been submitted previously, in whole or in part, for the award of any other academic degree or diploma.

I cede copyright of the thesis in favour of the University of Ecole Centrale De Nantes, France.

Date: 21st August 2022 Signature: 

Contents

List of Figures

List of Tables

List of Acronyms

BV	Bureau Veritas
CFL	Constant Fatigue Life
CFRP	Carbon Fibreglass-Reinforced Polymer
CoG	Centre of Gravity
DoF	Degree of Freedom
FEMAP	Finite Element Modelling and Postprocessing
FEM	Finite Element Model
FLDs	Fatigue Life Diagrams
FOWT	Floating Offshore Wind Turbine
FOWTP	Floating Offshore Wind and Tidal Power
FRP	Fiberglass-Reinforced Polymer
FSI	Fluid-Structure Interaction
GW	Giga Watt
IEC	International Electro technical Commission
JONSWAP	Joint North Sea Wave Analysis Project
MD	Multidirectional fibre
QTFs	Quadratic Transfer Functions
RAOs	Response Amplitude Operators
SN	Number of cycles to failure, N(S), when a material is repeatedly cycled through a given Stress range S
UD	Unidirectional fibre
WP4	Workplan 4

List of Symbols

A	cross sectional area of blade
A_c	cross section area of floating body
$A_{proj,B}$	planform area of the blade
α	heading angle
α_{rc}	relative current velocity incidence w.r.to floater heading
α_{rw}	relative wind velocity incidence with respect to floater heading
[B]	damping matrix coming from the radiation problem solution and added damping defined by the user
B_{linear}	linear damping matrix of 6X6 size
B_{quad}'	quadratic damping matrix of 6X6 size
$\emptyset_{Rj}$	radiation potential
C_T	thrust coefficient
C_x	Non-dimensionnel drag coefficients in Surge
C_y	non-dimensional drag coefficients in Sway
C_z	Non-dimensionnel drag coefficients in Yaw
CF_x	drag coefficients in surge
CF_y	drag coefficients in sway
CF_z	drag coefficients in yaw
dmp_{ij}	radiation damping
D	damage
D_m	damage in matrix
D_f	damage in fibre
ε	small parameter associated to wave steepness
E	elastic modulus of steel
ζj	motion displacement
F_Z	relative weight load vertical force components
F	rotor thrust load
F_B	buoyancy forces
f_2	ratio between the ultimate strength in the T direction and the ultimate shear strength
g	acceleration due to gravity

Hs	significant wave height
I_{yy}	second moment of area in Y-plane
I_{xx}	second moment of area in X-plane
J_{ij}	added inertia
K	hydrostatic stiffness matrix of 6X6 matrix size
[K]	stiffness matrix coming from the hydrostatic properties of the body or added stiffness due to the mooring system
K_{wp}^{h}	heave restoring stiffness
K_{wp}^{r}	roll restoring stiffness
K_{wp}^{p}	pitch restoring stiffness
K_{h}^{44}	partial change in heave stiffness due to small roll angle perturbation
K_{h}^{55}	partial change in heave stiffness due to small pitch angle perturbation
L	perpendicular length of floater
[L]	hydrostatic load
[LD]	linear damping load
[M]	inertia matrix of the body
$[M_A]$	water-added mass coming from the radiation problem solution
a_{ij}	added mass
M_z	drag moment components in Z-direction
m	coefficient giving the slope of the SN curve
N_B	number of blades
n_i	referenced number of cycles for each type of stress cycles
N_i	calculated allowable number of cycles for each type of stress cycles
$N_{R,i}$	number of cycles to failure for each layer, matrix, and fiber for given stress ratio
P	equivalent pressure load
ρ_{steel}	density of steel
ρ_{air}	air density
ρ_{water}	density of sea water
ρ_i	alternate stress ratio
[Q [D]]	quadratic damping load
R	stress ratio

S	mean wetted surface area
S_L	projected longitudinal wind area above waterline
S_T	projected transverse wind area above waterline
SF_f	safety factor for fibre
SF_m	safety factor for matrix
σ_1	stress in the fibre direction
σ_2	stress in the direction perpendicular to the fibre
σ_a	stress amplitude
σ_{alt}	alternate stress during the cycle
σ_{brt2}	theoretical breaking stress in tension in the transverse direction
σ_{brc2}	theoretical breaking stress in compression in the transverse direction
σ_f	fibre stress
σ_i	ratio of the theoretical breaking stress
σ_{max}	maximum stress
σ_{min}	minimum stress
σ_{mean}	mean stress during the cycle
σ_m	equivalent matrix stress
σ_{ucs}	ultimate compressive stress
σ_{ult}	ultimate tensile strength of steel
σ_{uts}	ultimate tensile stress
T	draft of floater
Tp	peak period
T_{period}	time for occurrence of one cycle
τ_{br12}	theoretical in-plane shear breaking stress
τ_{12}	the in-plane shear stress
$[U]$	motion vector of the body
$\vec{u}$	fluid velocity
$\overrightarrow{u_W}$	wind velocity on the inertial basis
$\overrightarrow{u_{rw}}$	relative wind velocity
$\overrightarrow{u_{rc}}$	relative current velocity
$v_x^{'}$	FOWT relative velocity with current projected in the X-direction
$v_y^{'}$	FOWT relative velocity with current projected in the Y-direction
V_a	wind intensity at the height z_a

V_{e50}	extreme wind speed
ϑ	Poisson ratio of steel
Δ	volume displacement
$\vec{v}$	floater velocity
$V(t)$	velocity of wind
$V(z)$	design wind speed
V_{gustN}	operating gust speed
W	weight of floating body
ω	angular velocity
X	ship state array
x_B	centre of buoyancy in x-coordinates
γ	peak enhancement factor
y_B	centre of buoyancy in y-coordinates
z_a	height of tower section from tower base
z_{hub}	height of hub from tower base
z_g	centre of gravity in z-coordinate
z_B	centre of buoyancy in z-coordinates

1. INTRODUCTION

Renewable energy exploitation from offshore has a significant growth potential. In recent years, there has been a steady increase in the capacity of offshore wind farms in Europe. In 2020, the growth of wind farms has been increased by 20% from 2019 with 34.4GW installed across the Europe [1]. It reduces the CO_2 emissions as well increase the Europe's technical and economic competitiveness. However, offshore energy production is subject to the harsh conditions of the open sea, which primarily impacts their installations and maintenance cost [2].

1.1 Motivation

For the past two decades, extraction of offshore wind energy has grown tremendously, primarily using monopile foundations and cylindrical shell towers made from steel [1]. With improved competitiveness and novel support structure concepts, the industry has built wind farms in shallow to intermediate water and deep-water locations despite the practical limitations of established construction methods [3].

It is becoming increasingly important to re-evaluate what type of support structure is most appropriate with increased oceans depths, the size and mass of turbines, and the increased tower height [1]. As structures become larger, steel's benefits diminish. For larger offshore wind turbine structures, self-weight plays a vital role in the design. Thus, selection of suitable material is necessary [1].

Composite materials such as carbon or glass fibre (FRP) are being considered as an alternative construction material to steel due to their potential benefits which are listed below [3].

1. Ensure corrosion resistance and fatigue resistance to ensure deterioration-free operation.
2. Reduce operating costs and improve efficiency through lighter weight.
3. Sound baffles achieve a less noisy work environment.
4. Flexibility in designing complex shapes.
5. Enhanced stiffness for improved stability.
6. Durable lighter-weight materials with a high strength-to-weight ratio.
7. Stable performance over time.

Though, FRP has superior properties, it has only been used in rotor blades [4]. The platform structure and turbine tower of FOWT is still made of steels [3]. The FIBREGY project proposed by the Enerocean aims to enable the use the of large of FOWTP platforms and turbine towers constructed with FRP materials [1]. The master thesis is a part of the FIBERGY project. The goal of FIBREGY will be achieved by developing, qualifying, and auditing innovative FRP materials for offshore applications by developing new design procedures and guidelines, and generating efficient production, inspection, monitoring methodologies, and validating and demonstrating with advanced software analysis tools[5].

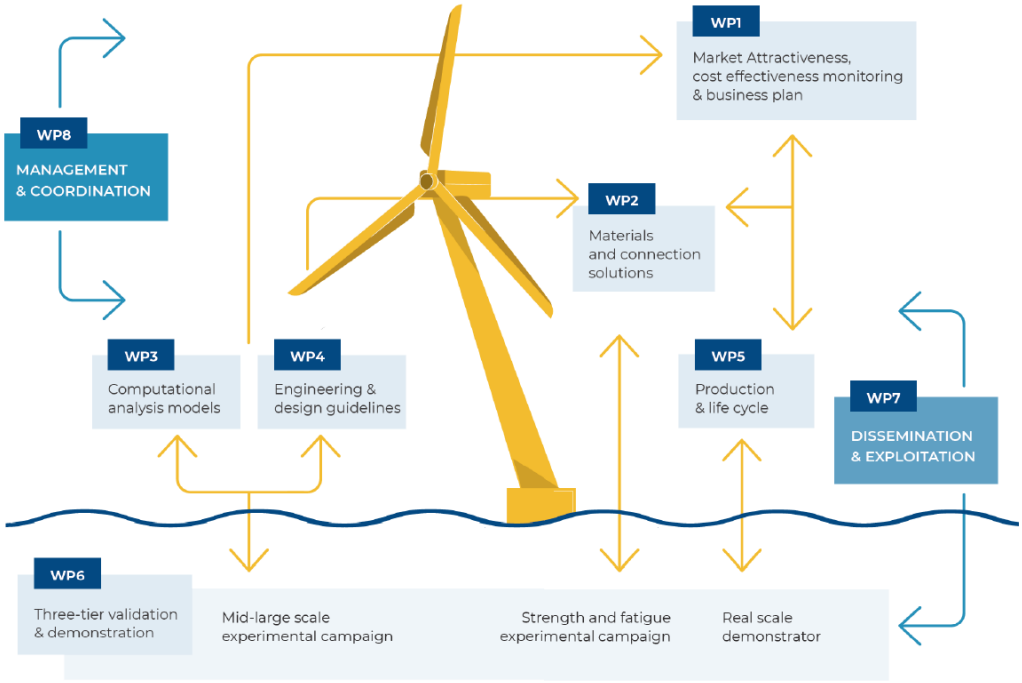

Figure 1-1. Workplan of FIBREGY

It focuses on six technical work packages: market attractiveness, cost-benefit analysis, and business plan; computational and analysis models; fibre-based materials and assembly solutions; design, engineering, and manufacturing guidelines; optimized production procedures; and technology validation [5]. Figure 1-1 [5] shows the different work packages.

The master thesis work on the fatigue assessment of the structure is one of the subsections of WP4. The work assigned to the WP4 is shown in Figure 1-2 [5].

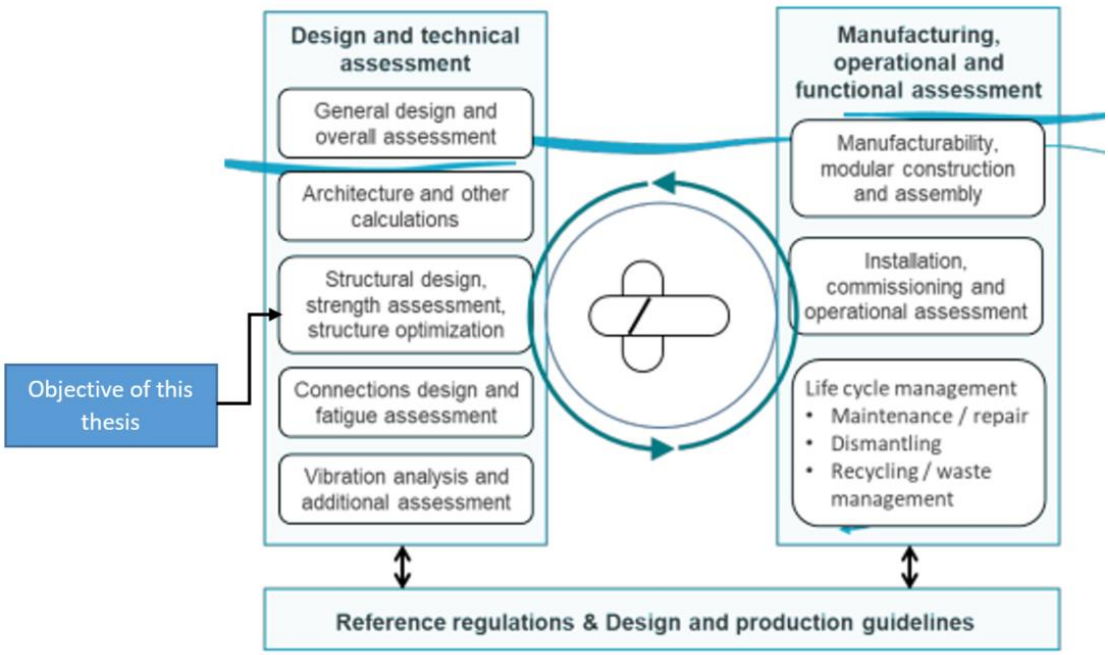

Figure 1-2. WP4 Section of FIBREGY

1.2 Organisation of the thesis

A brief introduction to the FOWT is provided in Chapter 1 of this document, and the work packages of the FIBREGY project are described in the application of composite materials to FOWT structures. A list of the potential benefits of composite materials over steel materials is also discussed. Chapter 2 describes the problem of fatigue that occurs in FOWT structures due to environmental loads, such as wind and waves. A discussion of the software used in the thesis and various segments of the work is presented in Chapter 3. An overview of the structural analysis is presented in Chapter 4. Bureau Veritas' fatigue methodology is discussed, which is used to assess the damage life of a structure. This section also explains the fluid-structure interaction principle. In Chapter 5 through Chapter 7, the work done on software FEMAP, ComposeIT, and OPERA is described. In Chapter 7, the hydrodynamic response of the platform is also discussed using HydroStar software. Chapter 8 presents the results and discussion associated with using Python. The last chapter in this thesis presents conclusions drawn from the work and discusses its limitations. In addition, the references are listed.

2 PROBLEM STATEMENT

This thesis aims to develop a methodology to analyse the Fatigue of the Floating Offshore Wind Turbine Tower and Platform made of Composite materials. FOWT are subjected to fatigue loads arising from several environmental conditions, such as wind, wave, and operational load, in which these systems are designed to operate [6]. The design of an FOWT attempts to maximize the power production by optimizing the rotor blade diameter and the rotor/nacelle control system to capture as much of the wind force as possible [7]. The design of the tower structure should be optimized, which is achieved generally by making it as light as possible [8]. The design of tower structures should consider fatigue critical details, crack initiation, and progression potential in all environmental conditions [8]. The static and dynamic response as well as the aerodynamic damping produced by the turbine rotor in the environment must be considered [7], [8]. The damage resulting from loading cycles must be characterized in the long-term stress history and implemented according to the fatigue performance estimation design philosophy, such as safe life, damage tolerance, or fail-safe [2].

Thus, it is vital to estimate the fatigue life accurately to ensure that the FOWT is well designed to function throughout its expected service life. By doing so, power production can be optimized [9]. The long-term stress range history is calculated based on the environment conditions [9]. These stress histories help for the fatigue life estimation as per the BV primary standards and guidelines relevant to the design of FOWT tower structures [10]. This report explores how material behaviour and load conditions affect fatigue resistance and life estimation.

3 METHODOLOGY

This section reports about the different fatigue methodology used in the analyses of composite materials. It also lists down all the software's used to perform the analysis. A brief explanation of each software used in this thesis is discussed below:

1) **FEMAP** (Finite Element Modelling and Postprocessing) is an engineering analysis program that creates finite element models for complex engineering problems ("pre-processing") and displays the results ("postprocessing") [11]. The Finite element method finds the behaviour of components, assemblies, or systems under a set of boundary conditions. As part of the design process, it is typically used to reduce the cost of prototyping and testing, evaluate distinctive designs and materials, and perfect the structural design. The calculations has been computed using the solver NASTRAN [11]. It is used to model and mesh the geometry and perform dynamic analysis.

2) **ComposeIT** is a software tool developed by BUREAU VERITAS (BV) that provides the detailed strength analysis of composite panels and stiffeners [12]. It helps to defined individual layers, combined layers, laminates, plates, stiffeners (standard or custom shapes), and loads on these structural elements [12]. In the thesis, it is used to decide mechanical properties of laminates transferred to FEMAP.

3) **HydroStar** helps to understand the wave-body interactions in three dimensions using 3D diffraction/radiation potential theory [13]. It incorporates multi-body interactions, sending speed effects, and fluid motion dynamics in tanks. It supports the evaluation of structures for wave loads, motions, accelerations, relative motions, and wave elevation in the first and second order [13]. It has been used to evaluate the hydrodynamic response of the platform.

4) **OPERA** is tool to support design verification and certification of floating units built by BV teams [14]. It is a static and dynamic solver which uses the knowledge of multi-physics: hydrodynamic, aerodynamic, and mooring, along with hydrodynamic couplings. It offers a fully integrated modelling solution that includes all floating wind turbine components, from defining mooring system to

turbine blades [14]. In this project, it has been used to define global structural response for environmental load on FOWT structure.

The work methodology needed in each of these software's is depicted in Figure 3-1.

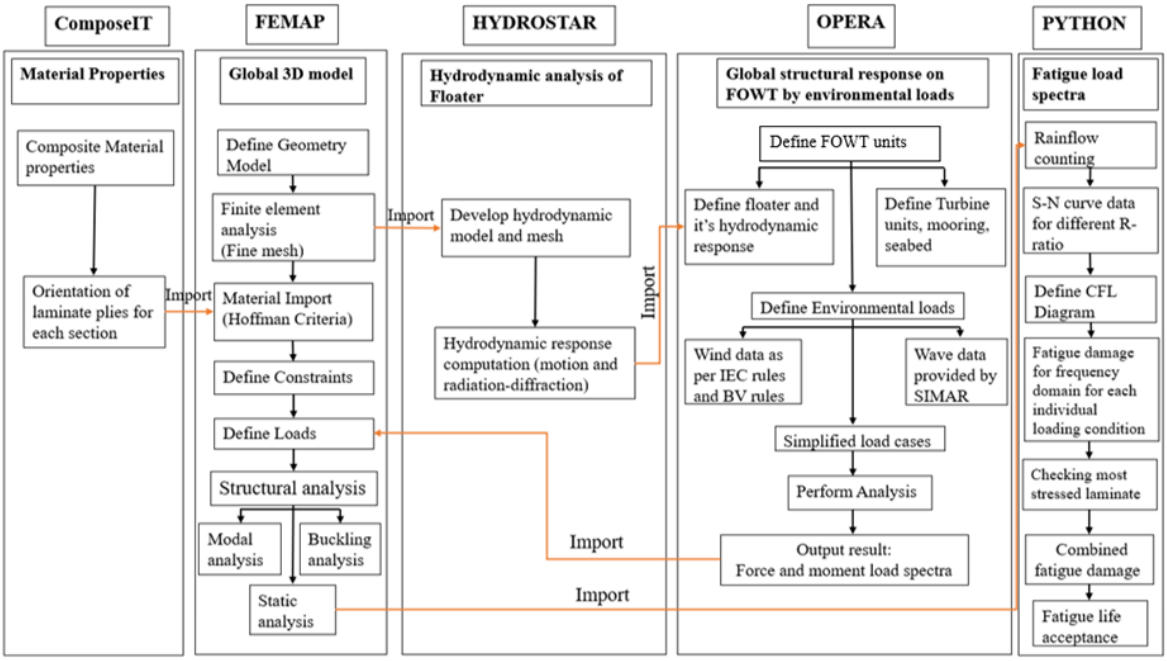

Figure 3-1. Methodology applied for fatigue study of FIBERGY Demonstrator

4 STRUCTURAL ANALYSIS THEORY

4.1 Fatigue Analysis

The fatigue analysis of FOWT structures is challenging. It requires significant planning and resources to model the wave, wind environments and simulate an integrated structural mode. A set of design fatigue factors such as Failure-safe design, damage-tolerant design, or safe life design can all be used to assess fatigue strength and estimate the FOWT's expected design life [7]. It is considered that the minimum design life of FOWT is 20 years, excluding the safety factor [3].

This section focuses primarily on three existing fatigue methodologies in the evaluation of fatigue life [10]:

1. Fatigue life models: It uses S-N curves or Fatigue Life Diagrams (FLDs) and predict only the final failure of the material.
2. Phenomenological models: It describe the fatigue evolution in terms of an empirical relationship with phenomena such as stiffness degradation.
3. Progressive damage models: It uses one or more damage variables, such as matrix cracks to quantify the extent of damage at each iteration.

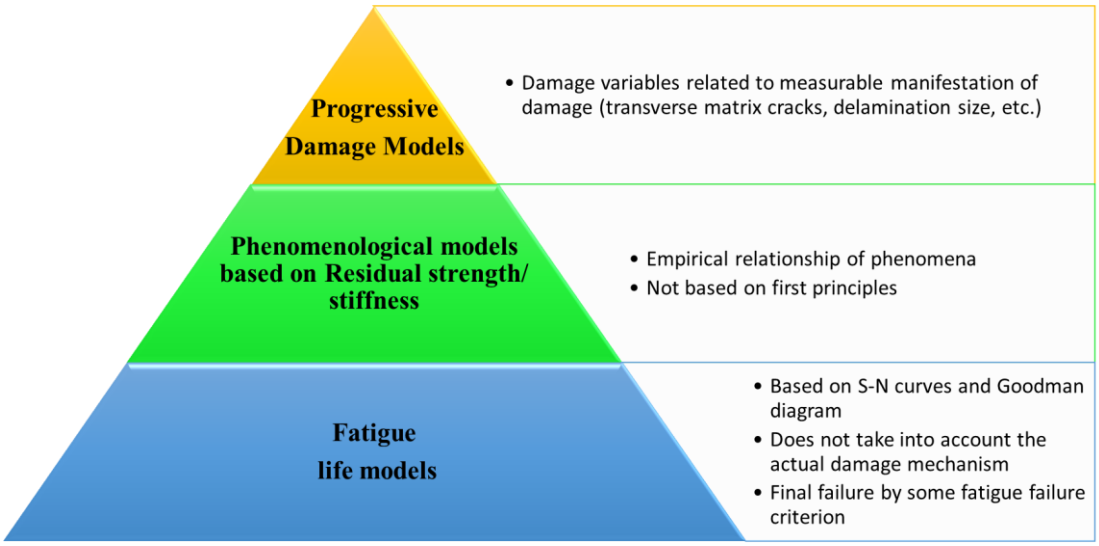

Figure 4-1. Existing fatigue methodologies

A schematic diagram showing above models are presented in Figure 4-1 [10] wherein the most basic model is placed at the base of the pyramid.

Progressive damage model is computationally expensive for complex loading conditions, especially at an early design stage [10]. Phenomenological models use the correlation with residual stiffness to evaluate the damage of composite material and thus computationally intensive [10]. However, in this thesis work, the fatigue life models are chosen to perform the derivation. It can be derived from multiple independent cycles of stress causing cracks to grow in structure [10]. The fatigue model relates damage accumulation to the number of load cycles depending on the loading conditions. In this model, S-N curves and fatigue failure criteria are used to calculate fatigue life [10].

4.1.1 Calculation of fatigue life using the fatigue life models

In this thesis, macro-mechanical laminate analysis tools from FEMAP are used to calculate the ply-by-ply stress for any given composite laminate. Figure 4-2 [10] below illustrates a graphical summary of the calculation procedure. The steps involved in the calculation of fatigue life is discussed below.

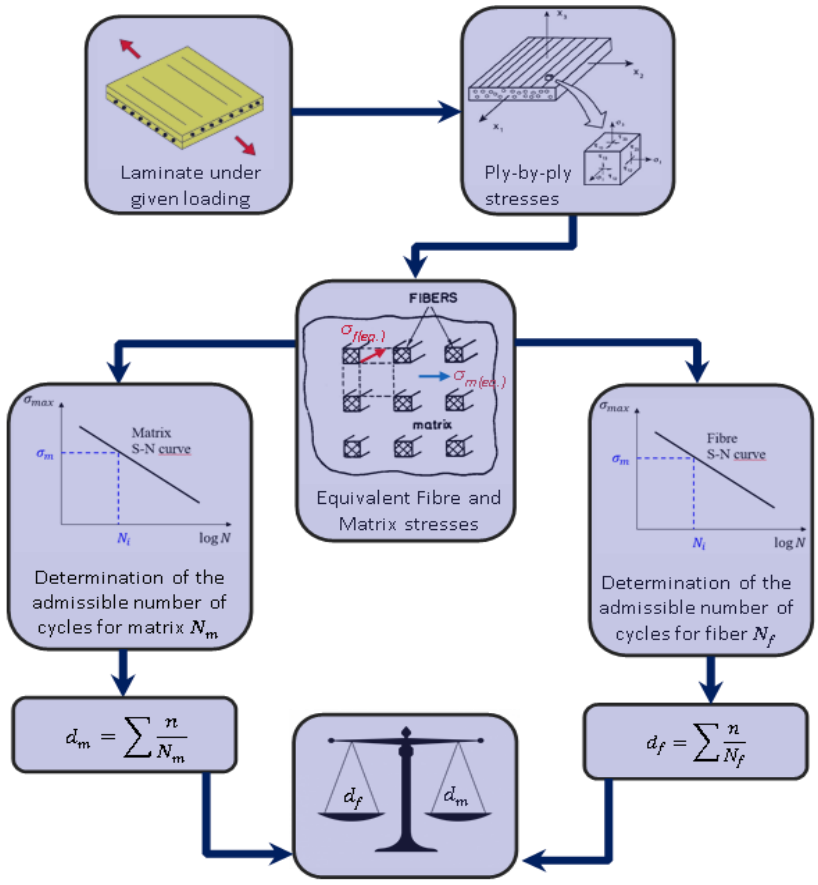

Figure 4-2. Procedure for fatigue life evaluati on using UD S-N curves

4.1.1.1 Evaluation of the fibre and matrix stresses

The first step is to evaluate the equivalent fibre and matrix stress for each ply. The NR546 BV Rules for Composite Materials sec 6 is taken into consideration for static calculation of a ply-by-ply stress decomposition [15]. It helps to find the local stress state $\sigma = [\sigma 1, \sigma 2, \tau 12]$ in each layer. The stress in different direction 1, 2, and 3 are depicted in Figure 4-2 [15].

where,

σ_1: the stress in the fibre direction (Normal X stress from FEMAP)

σ_2: the stress in the direction perpendicular to the fibre (Normal Y stress from FEMAP)

τ_{12}: the in-plane shear stress (Shear XY stress from FEMAP)

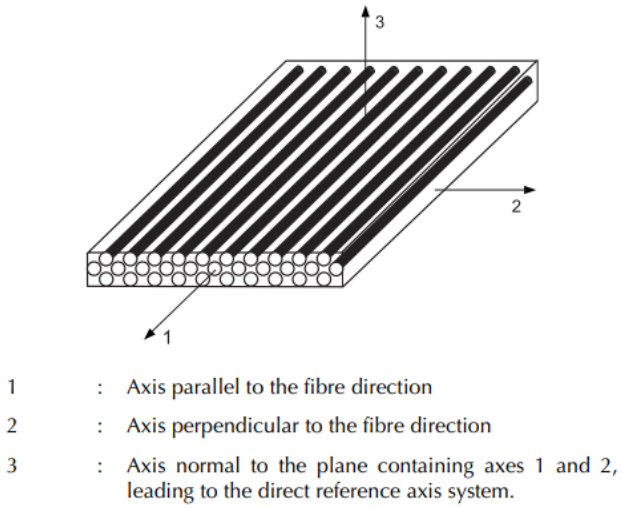

Figure 4-3. Composite material orientation

Determination of equivalent stress for matrix and fibre

The fatigue behaviour in the fibre and the matrix are assumed to be different [15]. Equivalent fibre and matrix stress σ_f and σ_m are defined to apply the methodology to both constituents of the composite material.

Equivalent fibre stress

Considering the equivalent stress in the fibre-dominated in direction 1, the effect of σ_2 and τ_{12} are ignored, while only the effect of σ_1 is taken as dominant and represented by (4.1) [10].

$$\sigma_f = \sigma_1 \tag{4.1}$$

Equivalent matrix stress

Equivalent matrix stress is calculated using the elliptical envelope failure formulation. It can be derived using almost any failure theory [10].

Mathematically, this can be computed as (4.2).

$$\sigma_m = \sqrt{\sigma_2^2 + (f_2\tau_{12})^2}, \quad Where\ f_2 = \begin{cases} \frac{\sigma_{brt2}}{\tau_{br12}} & if\ \sigma_2 \geq 0 \\ \frac{\sigma_{brc2}}{\tau_{br12}} & if\ \sigma_2 < 0 \end{cases} \tag{4.2}$$

4.1.1.2 Rainflow algorithm

After calculating the equivalent fibre and matrix stress, a python Rainflow-counting algorithms is used. It translates loading sequences with varying stresses into equivalent stress reversals with constant amplitudes as extreme peaks to calculate fatigue life [16].

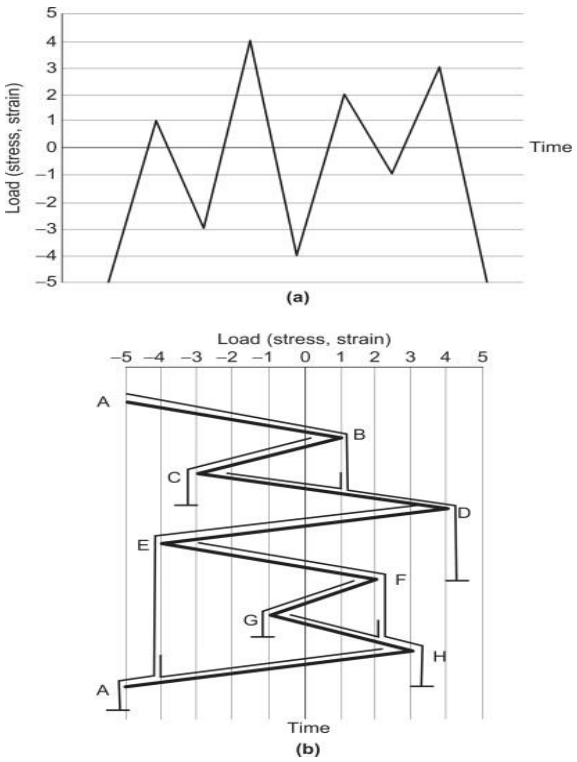

Figure 4-4. Rainflow Counting (a) and (b)

Here, In (Figure 4-4), every extreme peaks corresponds to a maximum stress value whereas lower valley corresponds to a minimum stress [16]. The difference between the maximum and minimum stress is termed as stress range. The ratio of minimum to maximum stress is known as stress ratio R [16].

Stress Ratio R

The stress ratio is essential to evaluate the number of loading cycles that the structure can sustain using the SN curve and is given by equation (4.3) [16].

$$R=\sigma_{min}/\sigma_{max}. \quad (4.3)$$

4.1.1.3 Design S-N Curves

A loading histogram is commonly used to describe multiple stress ratios and cyclic stresses in fatigue design applications [10]. SN curves behave differently for the composite materials for different stress ratios [10]. As the stress ratio changes, the slope of the SN curve will change [10]. Detailed information about the stress cycle history will be presented in the following subsection to find which S-N curves need to be considered. A formulation for SN curve is discussed below.

Formulation

The following equation (4.4) [10] defines the number of cycles to failure for each layer of matrix, and fibre.

$$N_{R,i} = \sigma_i^{-m} \quad (4.4)$$

where $\sigma_i=\sigma/\sigma_{br}$ is the stress level as the ratio of the theoretical breaking stress [10]. The breaking stress to be considered depends on the stress ratio R [10].

where,

$\sigma_{br}=\sigma_{brt}$, when $\frac{\sigma_{brc}}{\sigma_{brt}} \leq R<1$, and

$\sigma_{br}=\sigma_{brc}$, otherwise

Here, σ_{brt} and σ_{brc} is tension and compression, theoretical breaking stress respectively and m stands for the slope of the SN curve.

m Coefficient values

It depends mainly on the stress ratio and the type of material used [17]. Its value for carbon epoxy is defined for only few stress ratio [10]. Therefore, it is not possible to find the number of cycles for fatigue for different stress ratio using the SN curve. Thus, the CFL diagram is used to define the number of cycles for fatigue for different stress ratios R using interpolation [17]. Table 4-1 shows the coefficient values determined based on the work of Kawai and Itoh [10].

Table 4-1. Coefficient m-Slope of SN Curve

Fibre orientation	Axis Direction	R	Carbon Epoxy
UD	parallel to fibres	-1	23
		0.1	20
		10	50
	perpendicular to fibres	-1	11
		0.1	15
		10	165

4.1.1.4 CFL diagram

It is used to determine the mean and alternating stress for a given R defined for the number of cycles(N) [18]. An example of a fatigue life diagram is given in Figure 4-5 [18] where each line corresponds to an identical or constant fatigue life given for different stress ratios tested on (σ_{mean}, σ_{alt}) plane.

where,

$\sigma_{mean} = \frac{\sigma_{max}+\sigma_{min}}{2}$ is the mean stress during the cycle, and

$\sigma_{alt} = \frac{\sigma_{max}-\sigma_{min}}{2}$ is the alternate stress during the cycle

An example of CFL diagram constructed by taking S-N curves at different stress ratio is given below Figure 4-6.

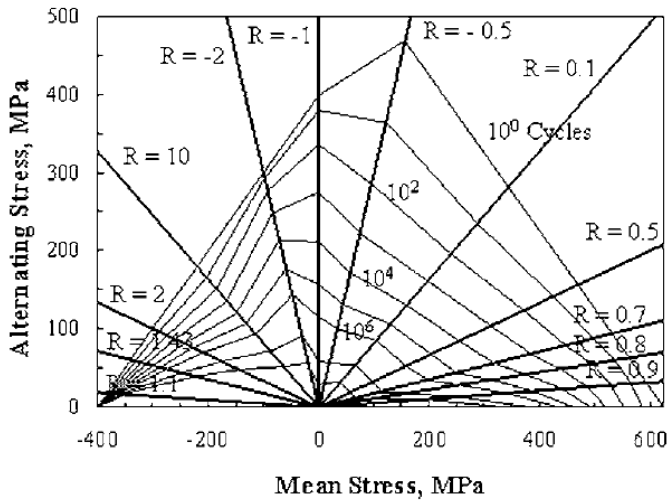

Figure 4-5. CFL Diagram

Based on two stress ratios (R1 and R3), the mean stress and stress amplitude corresponding to the same number of cycles (same fatigue damage state) for an intermediate ratio R2 can be obtained by linear interpolation as seen in Figure 4-6 [10].

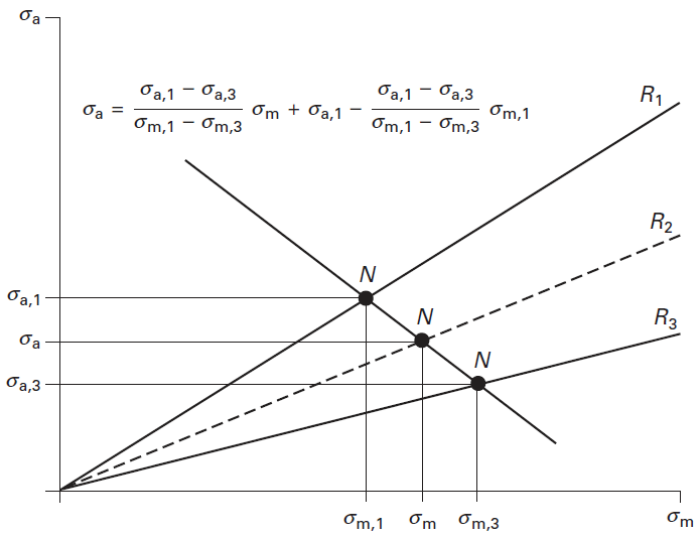

Figure 4-6. Mean stress v/s Alternating stress

The stress amplitude (σ_a) [10] for the intermediate ratio can be derived as:

$$\sigma_a = \frac{\sigma_{a1}(\rho_1 - \rho_3)}{(\rho_1 - \rho)\frac{\sigma_{a1}}{\sigma_{a3}} + (\rho - \rho_3)} \tag{4.5}$$

where ρ_i is the alternate stress ratio, defined as the ratio of the stress amplitude to the mean stress [10].

$$\rho_i = \frac{1 + R_i}{1 - R_i} \tag{4.6}$$

Equation (4.5) is only applicable if multiple stress ratio results are provided, which are not always available in most cases [10]. It is common to have results for one tensile stress ratio ($0<R<1$; $\rho>1$) and one compressive stress ratio ($R>1$; $\rho<-1$), as shown in Figure 4-6 [19].

In these cases, an extended case of (4.5) can be used to define the mean stress and stress amplitude [19] as:

$$\sigma_a = \frac{\sigma_{br}}{\frac{\sigma_{br}}{\sigma_{a1}} + \rho - \rho_1} \tag{4.7}$$

where $\sigma_{br}=\sigma_{uts}$ for tensile fatigue case or

$\sigma_{br}=\sigma_{ucs}$ for compressive fatigue case

Based on the interpolated SN curve, the number of allowable stress cycles can be found and used to evaluate the damage ratio.

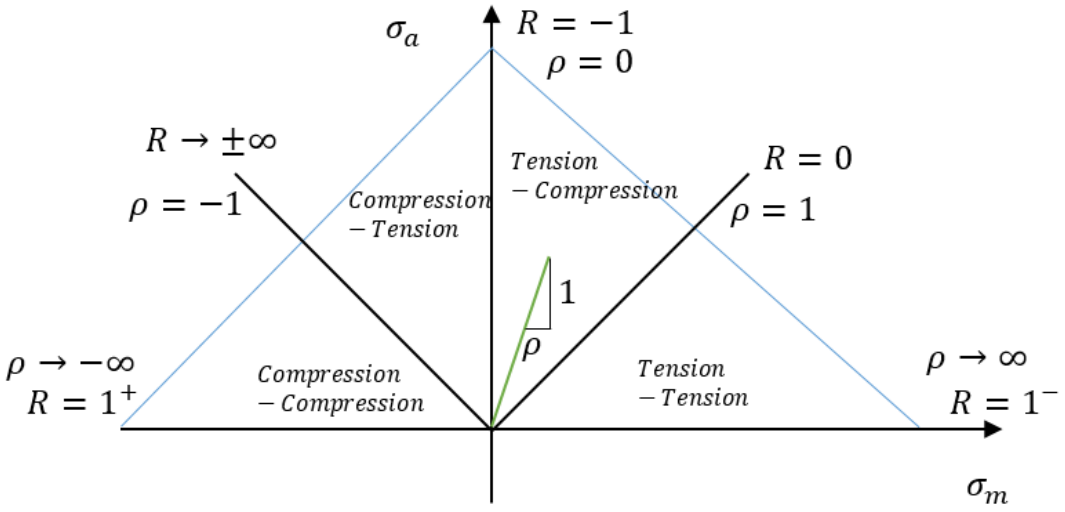

Figure 4-7. GOODMAN Analysis for R and ρ

4.1.1.5 Damage calculation

The fatigue structure assessment is based on the cumulative damage principle. The Miner's sum is used to calculate the total damage ratios [10] D_f and D_m for fibre and matrix using (4.8) and (4.9)

$$D_f=\sum_i \frac{n_{f,i}}{N_{f,i}} \tag{4.8}$$

$$D_m=\sum_i \frac{n_{m,i}}{N_{m,i}} \tag{4.9}$$

4.1.1.6 Criteria

The total damage ratios are to comply with the following formulas to ensure the safety of the material [10].

$$D_f\leq\frac{1}{SF_f} \tag{4.10}$$

$$D_m\leq\frac{1}{SF_m} \tag{4.11}$$

The safety factor SF_f and SF_m are to be determined based on failure-safe design, damage-tolerant design, or safe life design [10].

FEMAP, and ComposeIT softwares are used to obtain the stresses in each ply and Python script is used to obtain the fatigue damage in sections, 8.3 and 8.4.

4.2 Fluid-Structure Interaction

A fluid-structure interaction (FSI) is a multi-physics interaction between fluid dynamics and structural mechanics. In this phenomenon, fluids flow inside or around a deformable or moving structure, which can be stable or oscillatory [20]. As fluid flow encounters structures, it exerts stresses and strains that can cause deformations in the solid object [20]. Depending on the flow's pressure and velocity, and the structure's material properties, these deformations can be large or very small [20].

If the deformation is small and the change in time is also relatively slow, the structure's deformation will not affect the fluid's behaviour. Consequently, the solid parts should only be stressed due to the resultant forces [20]. Nevertheless, if the structure deforms large, the fluid's velocity and pressure fields will change, and we must consider this as a bi-directional coupled multi-physics problem: The fluid's flow and pressure affect the structure's deformation [20]. OPERA, and HydroStar software are used to know the encounters of fluid flow with the structure and discussed in section 7.1.

5 MODELLING OF GEOMETRY

FEMAP is used to create the finite element model of turbine tower.

5.1 Geometry

FIBREGY has two wind turbines mounted on a single floating semi-submersible platform as shown in Figure 5-1.

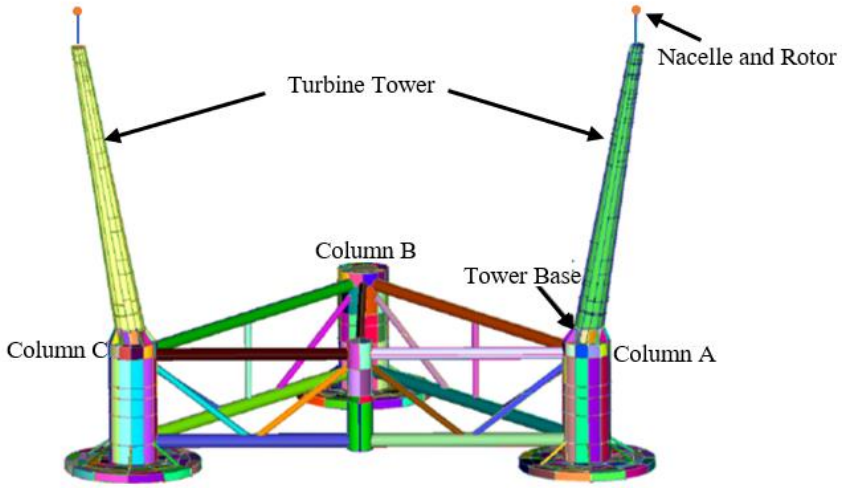

Figure 5-1. Twin Tower Wind Turbine Design

The platform comprised of three primary columns A, B, and C with heave plates on the bottom to provide buoyancy and damping [3]. A bracing system with horizontal and diagonal orientations hold these columns together, completing the platform model [3]. The platform model is further used for structural analysis using OPERA and HydroStar which are described in section 5.2.2 and 5.2.3.

An inclined turbine tower along with nacelle and the rotor is used for the modal analysis, and transient analyses in FEMAP. Pre-processing and post-processing are also performed with FEMAP.

5.2 Mesh properties

5.2.1 Mesh used in FEMAP

Multiple meshes (mesh in the quad) has been applied to verify the convergence and stability of the FEMAP analysis solution. In the equilibrium situation, a mesh size of

20mm is used. The convergence of the mesh result is shown in Appendix A. The Finite Element model of the tower is meshed using the Plate element type. The shape considered for mesh is a Quad element shape, while the top portion of the tower is considered a rigid body for rotor and nacelle, which can be seen in Figure 5-2.

For the simplicity of the study, the base of the tower is considered clamped i.e., all nodes are fixed (Figure 5-3).

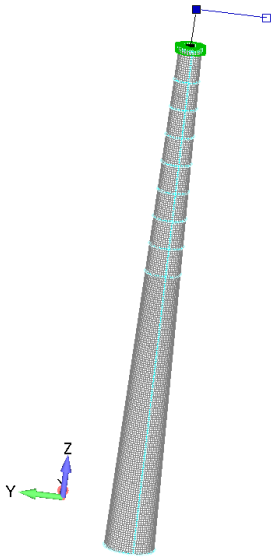

Figure 5-2. Turbine Tower Mesh

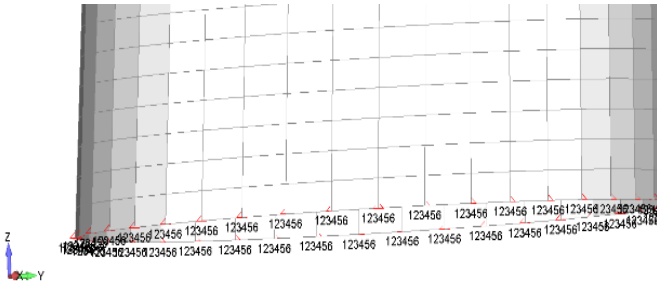

Figure 5-3. Constaints in FEMAP

5.2.2 Mesh used in OPERA

Figure 5-4 shows the mesh for the platform provided by the FIBREGY partners. This mesh is only used for the visual presentation of platform in OPERA [14].

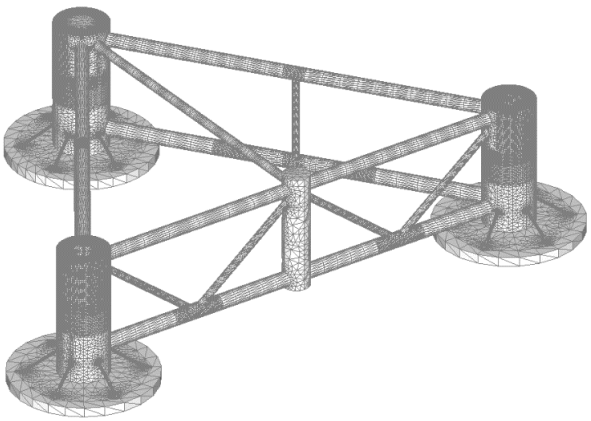

Figure 5-4. Floater mesh (Use in OPERA)

5.2.3 Mesh used in HydroStar

In HydroStar, only the draft part of platform mesh is used as shown in Figure 5-5. Due to the hydro mesh's actual limitation, the platform is discretized into a smaller number of nodes [13]. Additionally, it is checked and verified to ensure no error in it, such as inconsistency or a zero number of area panels can be seen in Appendix C. The braces connecting the heave plate with columns are tiny in size, which can't be modelled with potential solver software like HydroStar [13]. Thus, it is recommended to remove it in further calculation.

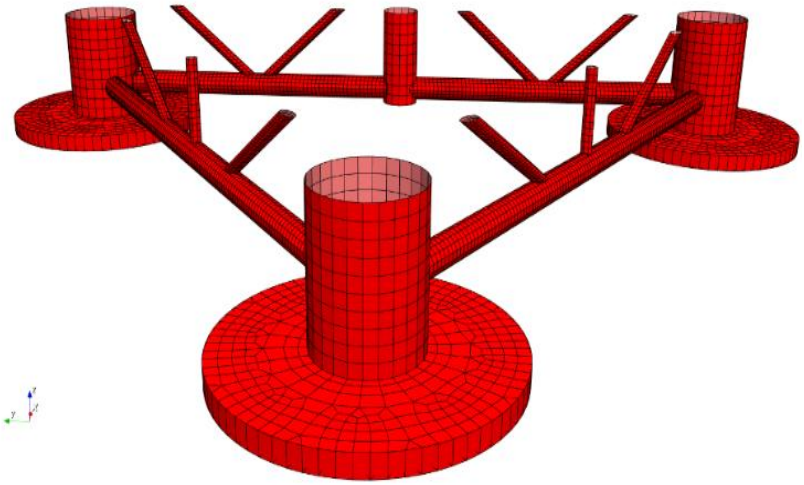

Figure 5-5. Mesh View in HYDROSTAR

6 IMPORT MATERIAL PROPERTIES (COMPOSEIT)

6.1 Material properties

Considering different multi-criteria matrices, weighting engineering, economic, and environmental properties, the material used for the laminate layout in this project is an epoxy resin composite with carbon fibre reinforced plastic (CFRP).

The CFRP material properties shown in Table 6-1, and Table 6-2 are based on the technical datasheets provided by the manufacturers and the experiment performed by the partner's company.

Table 6-1. Mechanical Characteristics of Carbon Epoxy UD

MECHANICAL CHARACTERISTICS (Carbon Epoxy UD)						
Thickness	0.514	mm		Relative Density	1.543	
Elastic Coefficients				**Breaking Stresses**		
E1	128410	Mpa		σ_{1T}	1387.00	Mpa
E2	6080	Mpa		σ_{1C}	982.00	Mpa
G12	3820	Mpa		σ_{2T}	55.00	Mpa
G13	3820	Mpa		σ_{2C}	126.00	Mpa
G23	3000	Mpa		τ_{12}	55.00	Mpa
ϑ_{12}	0.273			τ_{L1}	55.56	Mpa
ϑ_{21}	0.013			τ_{L2}	66.84	Mpa

Table 6-2. Mechanical Characteristics of Carbon Epoxy MD

MECHANICAL CHARACTERISTICS (Carbon Epoxy MD)						
Thickness	0.309	mm		Relative Density	1.543	
Elastic Coefficients				**Breaking Stresses**		
E1	130693	Mpa		σ_{1T}	1568.31	Mpa
E2	6302	Mpa		σ_{1C}	1110.89	Mpa
G12	4178	Mpa		σ_{2T}	63.02	Mpa
G13	4178	Mpa		σ_{2C}	144.94	Mpa

G23	3500	Mpa		τ_{12}	66.84	Mpa
ϑ_{12}	0.273			τ_{L1}	55.56	Mpa
ϑ_{21}	0.013			τ_{L2}	68.84	Mpa

Table 6-3 and Table 6-4 show the combined layer of carbon fibre 0º/90º and ±45º along with laminates properties:

Table 6-3. Combined Layer Carbon Epoxy 0º/90º MD

Carbon Epoxy 0/90 MD			
#	Layer Label	Angle (º)	Thickness (mm)
1	Carbon Epoxy MD	0.00	0.31
2	Carbon Epoxy MD	90.00	0.31
3	Carbon Epoxy MD	90.00	0.31
4	Carbon Epoxy MD	0.00	0.31
Laminate results			
Thickness (mm)	1.23	Weight (kg/m^3)	1.905
Fibre weight (kg/m^3)	1.200	Resin weight (kg/m^3)	0.705
Ex (MPa)	68701	Vx (mm)	0.617
Ey (MPa)	68701	Vy (mm)	0.617
Gxy (MPa)	4178	(EI)x (N/mm)	1.808E+4
ϑ_X	0.025	(EI)y (N/mm)	3.432E+3
ϑ_y	0.025	Density (g/cm^3)	1.543

Table 6-4. Combined Layer Carbon Epoxy ±45º MD

Carbon Epoxy +45/-45 MD			
#	Layer Label	Angle (º)	Thickness (mm)
1	Carbon Epoxy MD	45.00	0.31
2	Carbon Epoxy MD	-45.00	0.31
3	Carbon Epoxy MD	-45.00	0.31
4	Carbon Epoxy MD	45.00	0.31
Laminate results			
Thickness (mm)	1.23	Weight (kg/m^3)	1.905

Fibre weight (kg/m^3)	1.200	Resin weight (kg/m^3)	0.705
Ex (MPa)	14939	Vx (mm)	0.617
Ey (MPa)	14939	Vy (mm)	0.617
Gxy (MPa)	33509	(EI)x (N/mm)	2.144E+3
ϑ_x	0.788	(EI)y (N/mm)	2.144E+3
ϑ_y	0.788	Density (g/cm^3)	1.543

Different laminate layers are used in this composite material, including the MD fabric 0º/90º, MD fabric ±45º, and UD fabric. In UD fabric, 100% of the fibre tow is oriented at 0º. In MD fabric 0º/90º, 50% of the fibre tow is oriented at 90º while the other 50% is oriented at 0º. In MD fabric ±45º, 50% of the fibre tow is oriented at +45º while the other 50% is oriented at -45º.

The turbine tower is composed of a combination of carbon fibre UD and MD fabric to maximum of 38 plies to minimum of 26 plies. The tower section thickness taken into account varies linearly from the base to the top, which is supported by Figure 6-1, and Table 6-5. The number of layers of plies are removed on the upper half section as the cross section decreases to have greater ease for infusion process [3].

Table 6-5. Material Thickness for each section of tower

Laminates for Plate (Carbon fibre)	
Distance (mm)	Mean thickness (mm)
Up to 0.5L	14,61
0.5L-0.55L	14,1
0.5L-0.6L	13,48
0.6L-0.65L	12,86
0.65L-0.7L	12,35
0.7L-0.75L	11,73
0.75L-0.8L	11,11
0.8L-0.85L	10,6
After 0.85L	10,08

The material defined in ComposeIT is imported to the geometry model in FEMAP. These composite materials are oriented in the vector direction aligned to the structural height, as shown in Figure 6-2

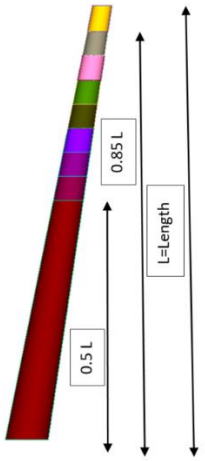

Figure 6-1. Material stacking for each section of tower

.

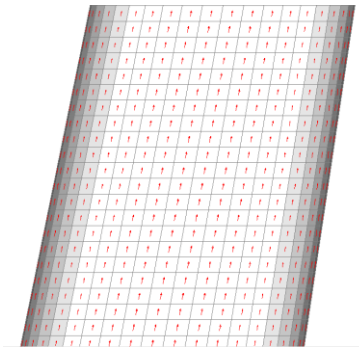

Figure 6-2. Orientation of composite materials in tower

For the rest of the structure corresponding to the connectors attached to the turbine tower's bottom section and platform, the material selected is S-355 steel, with the following mechanical properties, used in section 7.1.1.

Table 6-6 Material Properties of S-355 Steel

E	2.1e11 N/m^2
ϑ	0.3
ρ_{steel}	76.93 N/m^3
σ_{ult}	355 MPa

7 FLUID-STRUCTURE INTERACTION

OPERA and HydroStar are used to study the fluid structure interaction to evaluate the response of environmental load on structure.

7.1 OPERA

In OPERA, the floating structures is taken as a state for seakeeping and station keeping for any environmental load conditions aided by sea and wind waves [14].

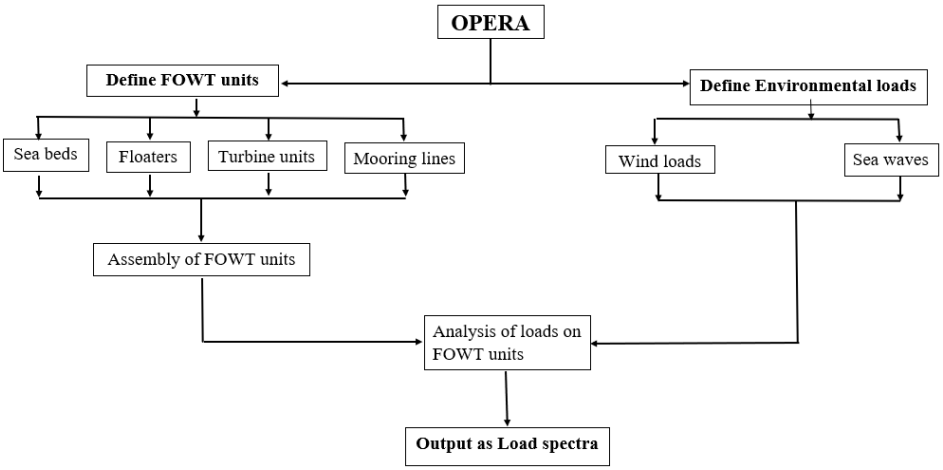

Figure 7-1. Opera work flow chart

The steps involved in defining the load time series for floating body are shown in Figure 7-1, and the description of each step is discussed below.

7.1.1 FOWT Units

7.1.1.1 Seabed

The floor of the sea or ocean is considered a seabed. It can be uniform or discrete according to the position. Although the seabed considered in FIBREGY project is discrete and varied with positions, due to the actual limitation of the OPERA software, the seabed considered here is uniform at the sea depth. The location of the seabed is essential to connect the mooring lines of the ocean bed to the floating structure. Three points are defined in the seabed to connect the mooring lines.

7.1.1.2 Mooring lines

The mooring system consists of three catenary mooring lines. Each mooring line at the column B has a pretension force acting on it. On the bottom of the heave plate, a

fairlead holds the platform at the bow during the simulation of anchoring. Figure 7-2, and Figure 7-3 show a schematic representation of these three anchor points, swinging circle radius and mooring footprint radius.

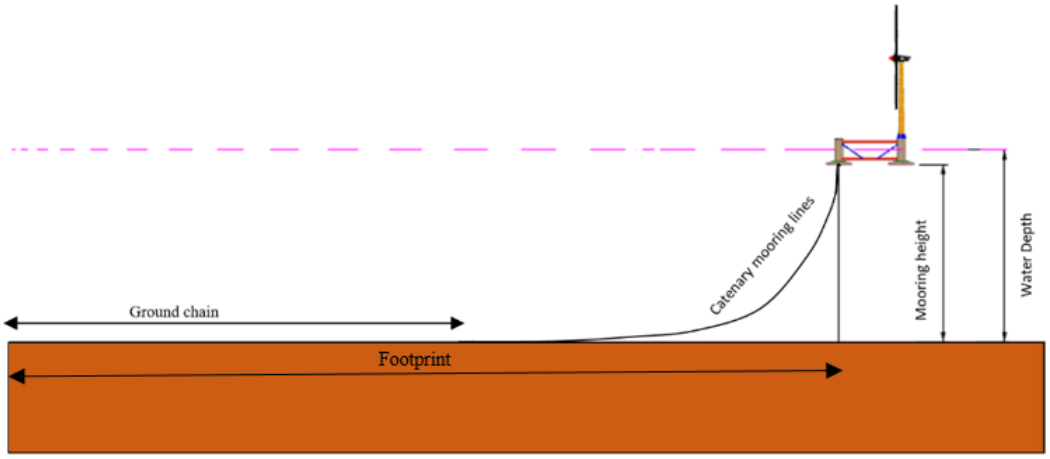

Figure 7-2. Catenary Mooring system

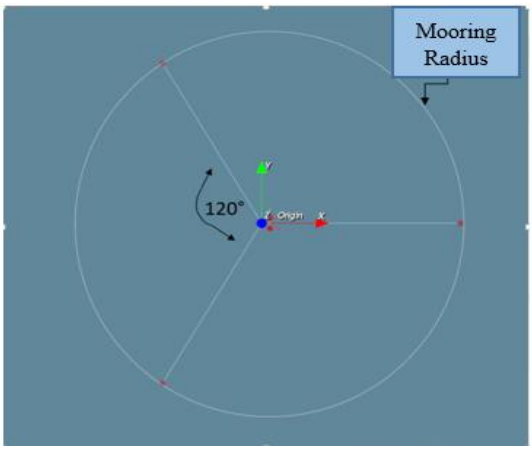

Figure 7-3. Swinging Mooring Circle Radius

OPERA calculates the individual characteristics of each mooring properties line by segmented lines approach [14]. Material properties and geometrical data about the segmented mooring lines (length, particular elements, seabed) are considered when calculating its characteristic. The movement of mooring lines is control by swivel.

The swivel absorbs the mooring system's vertical stresses and allows the structure to rotate in the wind's direction [3]. The platform rotates according to the wind direction to correctly position the wind turbines, as illustrated in Figure 7-4 [3].

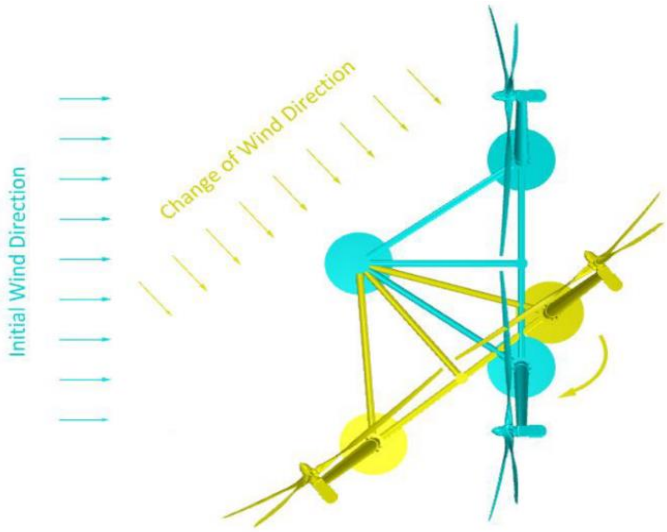

Figure 7-4. Swivel Action for Mooring Lines

Wave can interact with structure from different heading angles. Due to the swivel motion designed for the mooring system, the platform naturally rotates to face the waves [3]. If the wind comes from a different direction misaligned with the wave direction, the pitch control system is always designed to emulate the wind forces in 0º heading [3]. Therefore, the analysis performed in OPERA is for 0º heading angles only.

The mooring loads are calculated at the FOWTs gravity centre. The mooring lines are treated as slender bodies in OPERA, which calculates the tension exerted on the FOWT structure by interpolating distances using precalculated discretized characteristics [14]. During each simulation step, anchor-to-fairlead horizontal distances and azimuths are calculated for each line.

7.1.1.3 Turbine units

Turbine units form of following structures.

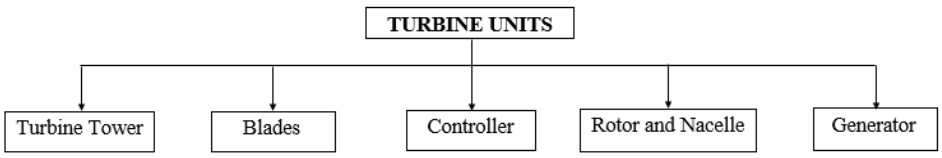

Figure 7-5. Turbine units

1) *Turbine Tower*

The turbine tower considered here is as same as in FEMAP. The linear mass, bending stiffness, axial stiffness, and torsional stiffness of each section in OPERA are evaluated with ComposeIT mechanical properties.

Two types of turbine tower analysis can be performed in OPERA.

i. Rigid Body Analysis

In this case, the tower is idealized not to deform or change in shape due to external loads acting on it. In this report, rigid body analysis of tower is considered.

ii. Flexible Body Analysis

In this case, the tower can be deformed by environmental loads acting on it. However, this analysis is not performed due to the actual limitation of OPERA.

2) Blades

Each wind turbine has three blades. Except for the mass of the blade, other data like unconstrained profile and associated stiffness are not available. Thus, the unconstrained profile of the blade for this project is modelled using the scale factors given the reference blade's data for a longer length. In OPERA, the blade element theory is taken into consideration. The blade is also considered as rigid body analysis in this thesis.

3) Controller

Wind turbine controllers consist of several computers that continuously monitor the wind turbine's status and collect statistics [21]. There are two methods for controlling the rotation of a wind turbine blade i.e., adjusting the generator speed or adjusting the blade angle [22]. FIBREGY project uses a pitch controller to adjust the blade angle. As the blades in wind turbines rotate, pitch controls adjust them to use the largest amount of wind energy possible while ensuring they do not exceed the maximum rotational speed.

Since the proper controller is unavailable during this thesis work. An alternative approach of applying the rotor thrust load directly is considered to keep the wind direction and rotor hub aligned. This might affect the realistic result that would have been possible if proper controller data has been used.

i. Rotor thrust load:

The thrust load (F) [23] is exerted on rotor as a punctual force by wind related with function of time given as:

$$F(t)=\frac{1}{2}\rho_{air}AC_TV(t)^2 \tag{7.1}$$

where C_T=thrust coefficient with a value of 0.5

Since the wind speed is not constant for one complete cycle, the equation used for the calculation of the variation in wind speed for a given period cycle [23] as:

$$V(t)=\begin{cases} V(z)-0.37V_{gustN}.\sin\left(\frac{3\pi t}{T_{period}}\right).\left(1-\cos\left(\frac{2\pi t}{T_{period}}\right)\right), & 0\leq t\leq T_{period} \\ V(z), \quad t<0 \text{ and } t>T_{period} \end{cases} \tag{7.2}$$

When the velocity given by the partners of FIBREGY (Figure 7-6) has been used, the displacement of the tower shows more oscillation. It is because there is no wind velocity initially, and suddenly there is a high wind velocity, which is unrealistic since the model does not assume damping.

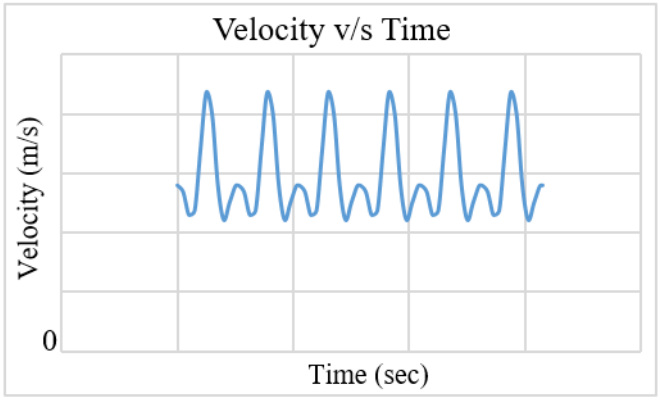

Figure 7-6. Velocities v/s time (Transient)

To eliminate the unnecessary oscillations, the velocity is shown to be increasing steadily (Figure 7-7) for a brief time. After a brief period of steady velocity increase, a transient response is considered.

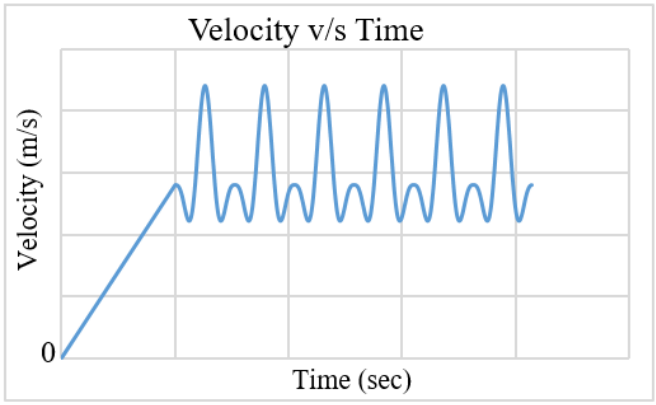

Figure 7-7. Velocities v/s time (Linear & Transient)

Using the above velocity wind profile, the thrust load calculated using (7.1). The Figure 7-8 shows thrust load applied at the rotor hub varied with time.

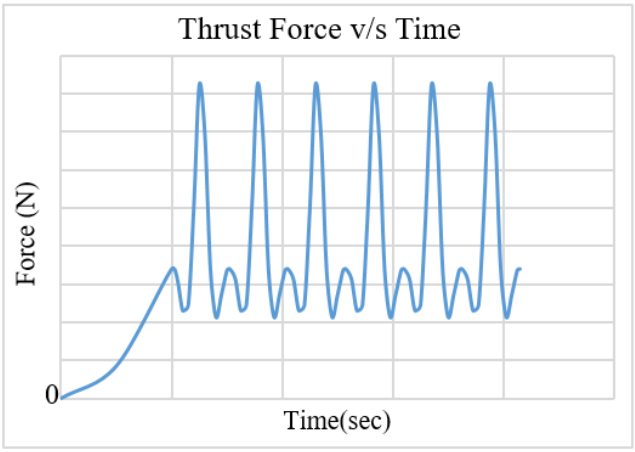

Figure 7-8. Time variation of thrust load

In Figure 7-8, the thrust force can be seen aligned with the square of velocity with similar nature of graph (Figure 7-7). It can be differed according to the environment condition considered from normal operating condition to extreme operating condition as seen in 7.1.3.

4) Other Turbine Units

The other turbine units considered here are Nacelle, Rotor Hub, and Shaft/Generator. Due to lack of data, the mass and CoG of these components are only taken into action.

7.1.1.4 Floater/Platform

In OPERA, the floater is imported as mesh defined in section 5.2 for visualization purposes only. To connect the opposite ends of mooring lines and tower connections, the mesh should be well made.

Various loads have been assigned to the floater, as mentioned in Table 7-1. Combination of these loads allow for creating different load cases necessary for correct analysis.

Table 7-1. Loads consider for Floater

Loads consider for Floater
Gravity load
Maneuverability load
Linear hydrostatic load
Relative current drag load
Relative wind drag load
Linear damping load
Quadratic damping load
1st order wave load with radiation
Archimedes load
2nd order wave load (QTF)

1) *Gravity load*

i. Material: Each structure part carries its weight load. This method has been applied to the entire geometry, considering the different densities of steel and FRP.

ii. Ballast: This load corresponds to the hydrostatic pressure in each column. Pressure is applied to the bottom plates of the heave plates by the ballast weight [3]. Accordingly, the load applied corresponds to the ballast required for obtaining the design trim and design draft of the platform [3]. In all cases, the ballast loads will be fixed, whose values are based on the final weight of the structure and the mooring tension [3].

iii. Rotor and Nacelle: Partners supply mass of nacelle and rotor.

Total light weight of platform is summation of all above mentioned loads. Partners provide this load. The design draft shows the displacement (Δ) based on the light weight and the dead weight. This displacement is used to evaluate the Archimedes load [3] using (7.3).

$$Archimedes\ load = \rho \Delta g \tag{7.3}$$

Thus, the relative weight load components F_Z [3] is calculated as:

$$F_Z = Gravity\ load - Archimedes\ load \tag{7.4}$$

2) Linear Hydrostatic Load

This load is considered for every floating or immersed body in a fluid. It is the force exerted by the water below the draft line and the vertical pressure exerted by the water height, as shown in Figure 7-9 [24]. It is loaded in the OPERA "Hydrostatic stiffness" section with a specific water weight of 1025kg/m^3. A displacement perturbation to the platform DoF consistent with each column index can be used to obtain each column of the hydrostatic stiffness matrix at once.

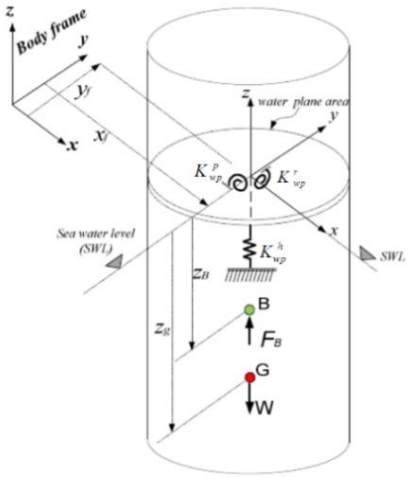

Figure 7-9. Buoyancy restoring force and moments at zero rotation angles

The hydrostatic load is given by (7.5)[24].

$$[L] = -[K][X] \tag{7.5}$$

$$K=\begin{bmatrix} 0 & 0 & 0 & 0 & 0 & 0 \\ 0 & 0 & 0 & 0 & 0 & 0 \\ 0 & 0 & K_{wp}^{h} & K_{wp}^{h}y_f & -K_{wp}^{h}x_f & 0 \\ 0 & 0 & K_{wp}^{h}y_f & K_{h}^{44} & -K_{wp}^{h}x_f y_f & (W-F_B)x_f \\ 0 & 0 & -K_{wp}^{h}x_f & -K_{wp}^{h}x_f y_f & K_{h}^{55} & (W-F_B)y_f \\ 0 & 0 & 0 & 0 & 0 & 0 \end{bmatrix} \quad (7.6)$$

where,

K= hydrostatic stiffness matrix of 6X6 matrix size,

X= [x, y, z, θ, ∅, φ] ship state array,

$K_{wp}^{h}=\rho g A_c$, termed as heave restoring stiffness,

$K_{wp}^{r}=\rho g I_{xx}$, termed as roll restoring stiffness,

$K_{wp}^{p}=\rho g I_{yy}$, termed as pitch restoring stiffness,

$K_h^{44}=-Wz_g+F_Bz_B+K_{wp}^{r}+K_{wp}^{h}y_f^2$, defined as a partial change in heave stiffness due to small roll angle perturbation,

$K_h^{55}=-Wz_g+F_Bz_B+K_{wp}^{p}+K_{wp}^{h}x_f^2$, defined as a partial change in heave stiffness due to small pitch angle perturbation, and

$F_B=-\rho g A_c$, is termed as buoyancy force

Hydrostatic forces do not affect surge and sway. Furthermore, there is no yaw moment. As a result, the value of first two rows, first two columns and last row are zero.

3) Drag Load

Fluid drag loads are applied to the FOWT in the inertial basis horizontal plane. Drag coefficients is defined in OPERA to a FOWT heading (α) angle. These coefficients are $CF_x(\alpha)$ in surge, $CF_y(\alpha)$ in sway, and $CF_z(\alpha)$ in yaw. These drag loads are due to current and wind waves [14].

i. Relative Current Drag Load and Relative Wind Drag Load:

Considering $\vec{v}$ as the floater velocity, $\overrightarrow{u_c}$ as current velocity, and $\overrightarrow{u_W}$ as wind velocity on the inertial basis, the three relative drag load components [14] F_x, F_y, M_z can be defined as:

$$F_x=CF_x(\alpha_r)u_r^2 \quad (7.7)$$

$$F_y = CF_y(\alpha_r)u_r^2 \tag{7.8}$$

$$M_z = CM_z(\alpha_r)u_r^2 \tag{7.9}$$

where,

$\alpha_r = \alpha_{rc}, u_r = u_{rc}$ for relative current drag load or

$\alpha_r = \alpha_{rw}, u_r = u_{rw}$ for relative wind drag load

Above mentioned coefficients are dimensional, respectively, with the units of kg/m, kg/m, and kg. To relate these dimensional coefficients with non-dimensional coefficients [14], following relation is used.

For relative current drag load:

$$CF_x = \frac{1}{2}\rho_{water} LTC_x \tag{7.10}$$

$$CF_y = \frac{1}{2}\rho_{water} BTC_y \tag{7.11}$$

$$CM_z = \frac{1}{2}\rho_{water} L^2 TC_z \tag{7.12}$$

For relative wind drag load:

$$CF_x = \frac{1}{2}\rho_{air} S_L C_x \tag{7.13}$$

$$CF_y = \frac{1}{2}\rho_{air} S_L C_y \tag{7.14}$$

$$CM_z = \frac{1}{2}\rho_{air} S_L C_z L \tag{7.15}$$

These non-dimensional coefficients depend on the shape of the floater at given heading angle. As the heading angle changes, the value of these coefficients changes for a given shape, which is recorded from the decay experiments. In this project, the heading angle considered is 0º and the value of coefficient [1] considered for relative current drag and wind load is presented in Table 7-2 and Table 7-3.

For relative current drag load:

Table 7-2. Current drag coefficient

Heading angle	C_x	C_y	C_z
0º	1	0	0

For relative wind drag load:

Table 7-3. Wind drag coefficient

Heading angle	C_x	C_y	C_z
0º	0.5	0	0

4) Damping Load

The damping load is applied to a floater, moving linearly with a velocity v and with an angular velocity ω. If [V] = [v_x, v_y, v_z, ω_x, ω_y, ω_z] is the floater velocity array, then the linear damping load [L [D]] [13] can be given as:

$$[LD] = -[B_{linear}][V] \quad (7.16)$$

where B_{linear}= linear damping matrix of 6X6 size

and the quadratic damping load [Q [D]] [13] is given as,

$$[Q\,[D]] = -[B_{quad}'][V^2] \quad (7.17)$$

where B_{quad}'= quadratic damping matrix of 6X6 size

Since the linear and quadratic damping coefficient can only be determined using the decay test [14]. Without any experimental data, it is not possible to figure out it accurately. Thus, values for linear and quadratic damping coefficient provided by project partners are used.

5) Manoeuverability Load

Manoeuverability loads are generated by the motion of a vessel based on hydrodynamics. It is calculated at the FOWT gravity centre, where the hydrodynamic load is composed of all the equation components based on linear and angular velocities [14]. Based on the input provided, manoeuverability load is calculated by OPERA.

6) Hydrodynamic load

The hydrodynamic loads used in the analysis for the platform are calculated using HydroStar. The results obtained are then imported into OPERA. The list of the hydrodynamic parameter used in OPERA is given below:

1. First order loads (including multi-bodies coupled terms)
2. Second order loads: Newman approximation (Full QTF loads)
3. Added mass for low and infinite frequencies (Radiation/Diffraction)

The hydrodynamic loads are defined in the software HydroStar which is explained below.

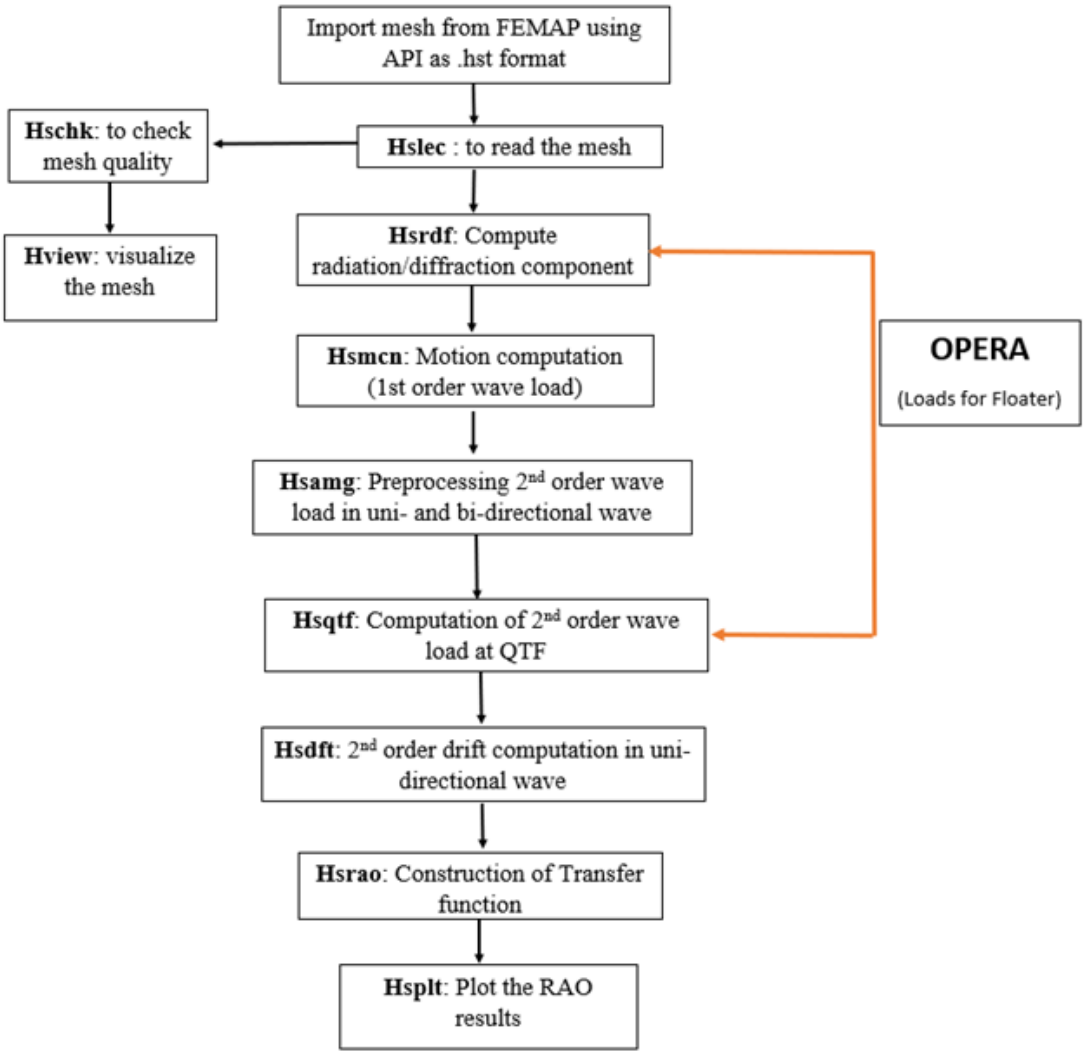

Figure 7-10. HYDROSTAR Work Flow Chart

i. <u>Radiation/Diffraction Load:</u>

Radiation solutions refer to the potential flow around the vessel when it moves in a quiescent fluid [13]. The radiation forces are composed of a term proportional to the body acceleration and another proportional to the body velocity. If ω is the wave frequency, ζj is the motion displacement, and j=1,2,3,4,5,6 corresponds to surge, sway, heave, roll, pitch, and yaw respectively, then the total radiation force [13] can be written as (7.18).

$$F_i = \sum_{j=1}^{6} \zeta_j(\omega^2 a_{ij} + i\omega\, dmp_{ij}),\ i=1,2,\ldots,6 \tag{7.18}$$

Here, a_{ij} refers to the added mass which sum up the system inertia.

$$a_{ij} = \rho_{water} \int \boldsymbol{R}_e \varnothing_{Rj}\, n_i dS \tag{7.19}$$

The added mass value can be obtained by solving six elementary radiation problems.

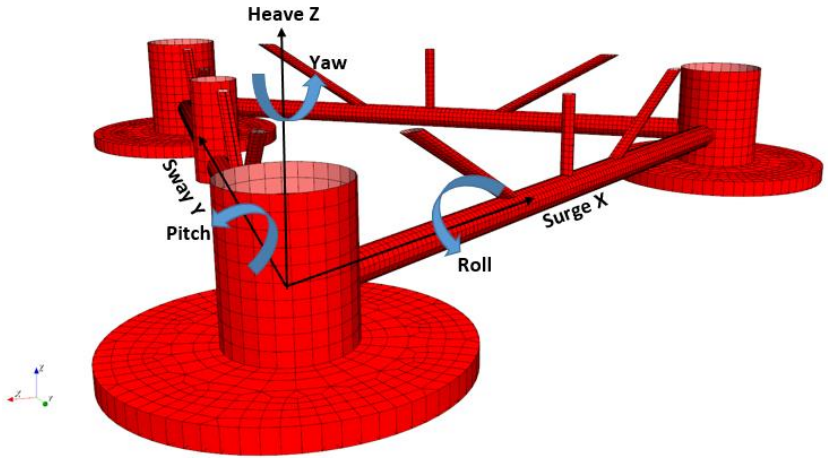

Figure 7-11. 6 DoF of FOWT

The added mass matrix is given by:

$$\begin{bmatrix} a_{11} & a_{12} & a_{13} & a_{14} & a_{15} & a_{16} \\ a_{21} & a_{22} & a_{23} & a_{24} & a_{25} & a_{26} \\ a_{31} & a_{32} & a_{33} & a_{34} & a_{35} & a_{36} \\ a_{41} & a_{42} & a_{43} & a_{44} & a_{45} & a_{46} \\ a_{51} & a_{52} & a_{53} & a_{54} & a_{55} & a_{56} \\ a_{61} & a_{62} & a_{63} & a_{64} & a_{65} & a_{66} \end{bmatrix}$$

where, a_{11}=added mass in surge direction

a_{22}=added mass in sway direction

a_{33}=added mass in the heave direction

a_{44}=added mass in the roll direction

a_{55}=added mass in the pitch direction

a_{66}=added mass in the yaw direction

The diffraction and radiation velocity potential are evaluated using HydroStar by the hsrdf module as shown in Figure 7-12 and Figure 7-13.

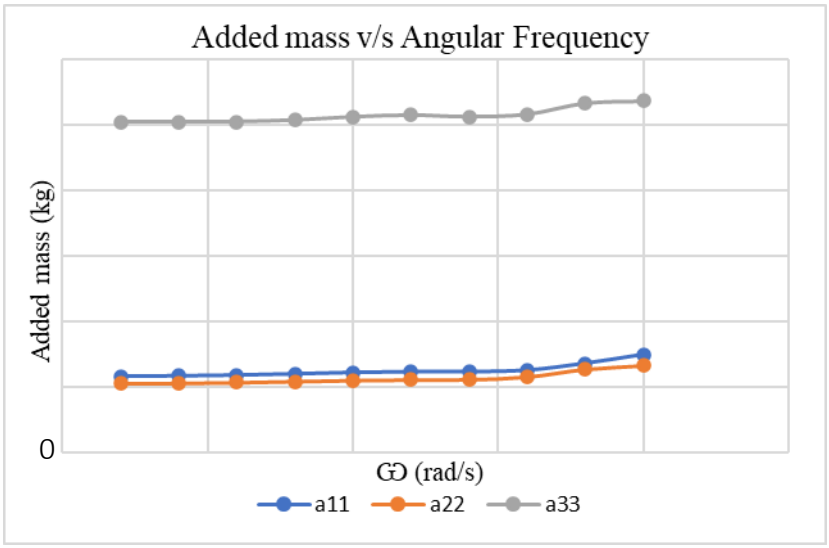

Figure 7-12. Added mass v/s Angular Frequency for surge, sway and heave

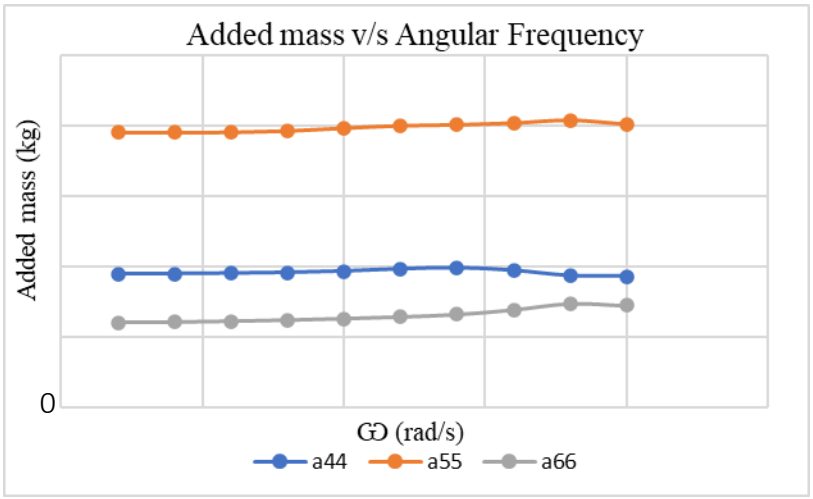

Figure 7-13. Added mass v/s Angular Frequency for roll, pitch and yaw

Figure 7-12 show that added mass due to heave motion is higher than that of surge and sway. It is due to the larger heave plate attached to the columns. It displaces more mass of water than the other two DoF. The added mass by surge and sway is same due to the symmetry of the structure.

Similarly, the added mass due to pitch motion is higher than the other two roll and yaw, as shown in Figure 7-13. This behaviour is due to the involvement of one heave plate at the front and two rear heave plate for the water displacement in pitch motion, while only two plates are involved for roll.

The parameter dmp_{ij} in (7.18) defines the radiation damping proportional to the velocity. The radiation damping is the resisting force to outcome the wave energy exerted on the structure due to wave-structure interaction. The formulation to evaluate the radiation damping [13] is given as:

$$dmp_{ij}=\rho_{water}\omega \int I_m \varphi_{Rj} n_i dS \tag{7.20}$$

Figure 7-14 illustrates the damping force exerted by the translational motion of the FOWT to compensate the force acted on it. The radiation damping is more in the heave motion than that of other two DoF as shown in the Figure 7-14. This can be explained by the presence of three heave plates attached to the column to oppose the motion in heave direction. The surge and sway motion exhibit same nature of radiation damping because of symmetry like added mass. In pitch and yaw, all three plates engage in damping, thus the value is greater. It is because the centre of gravity is not placed exactly at the central position.

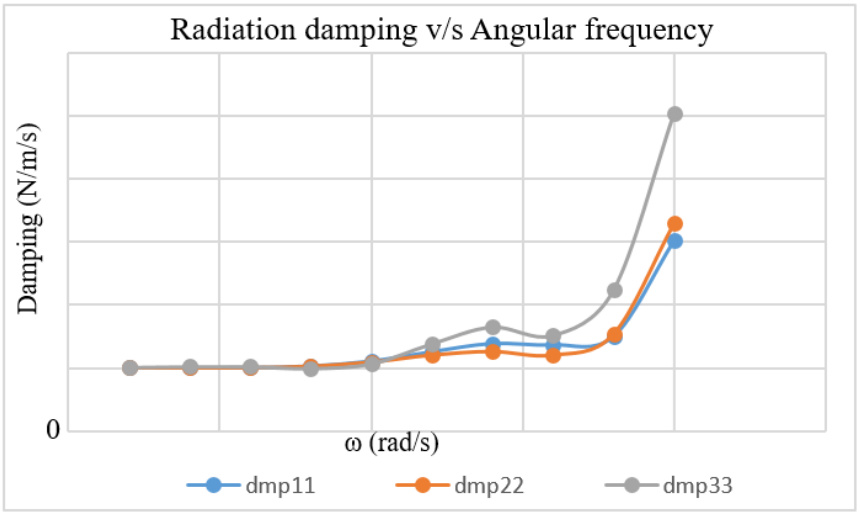

Figure 7-14. Radiation damping v/s Angular Frequency for surge, sway and heave

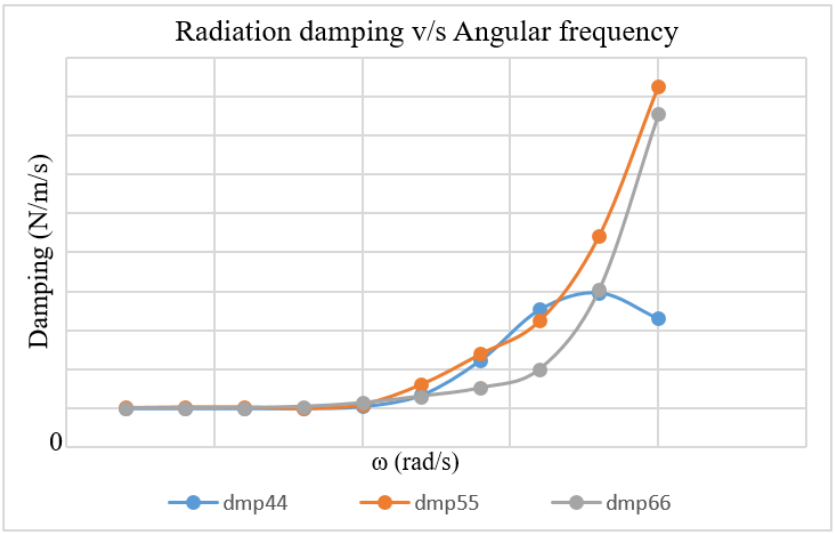

Figure 7-15. Radiation damping v/s Angular Frequency for roll, pitch and yaw

ii. 1st Order Wave Load:

Wave incident load is the first order load. It considers both linear and nonlinear parts [14]. In a physical sense, this force [14] can be modelled as

$$F=F^{(0)}+\varepsilon F^{(1)}+\varepsilon^{(2)}F^{(2)}+\varepsilon^{(3)}F^{(3)}+\ldots \quad (7.21)$$

where,

$\varepsilon F^{(1)}$ is the linear response

$\varepsilon^{(2)}F^{(2)}$ is the contribution of second order approximation

The only part considered in the first-order wave load is up to the linear response. Here, the induced phenomena such as load, or body motions occur at wave frequency. In HydroStar [13], Newton's Second Law was applied to describe the motions of floating bodies, and the following motion equation was derived.

$$([M]+[M_A])\ddot{U}+[B]\dot{U}+[K]U=F \quad (7.22)$$

The parameters in (7.22) are provided as an input in the prompt file in the HydroStar to compute the first order wave load. Figure 7-16, and Figure 7-17 represent the first order harmonic force and first order harmonic moment on the platform structure, respectively. In Figure 7-16, the force acted on the body due to surge direction increases with the increase in angular frequency and then decreased to a frequency called a cancellation period and afterward increases again. At this cancellation point, either the first wave

produced in the structure is cancelled entirely or is enormously decreased. The forces in sway and moments in X and Z-direction is zero because of symmetry.

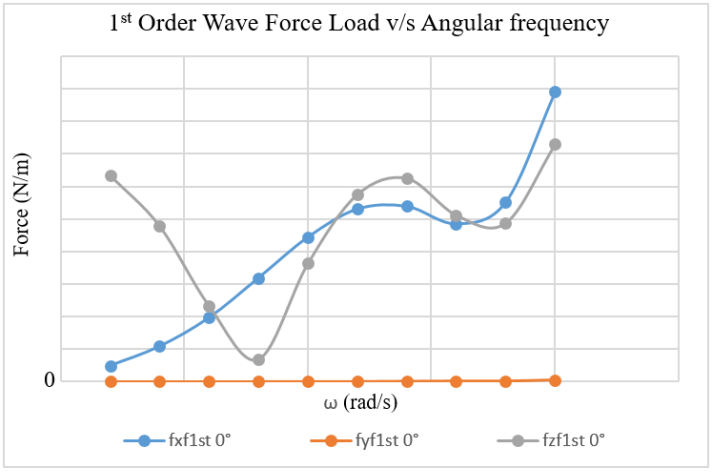

Figure 7-16. 1st Order Wave Load

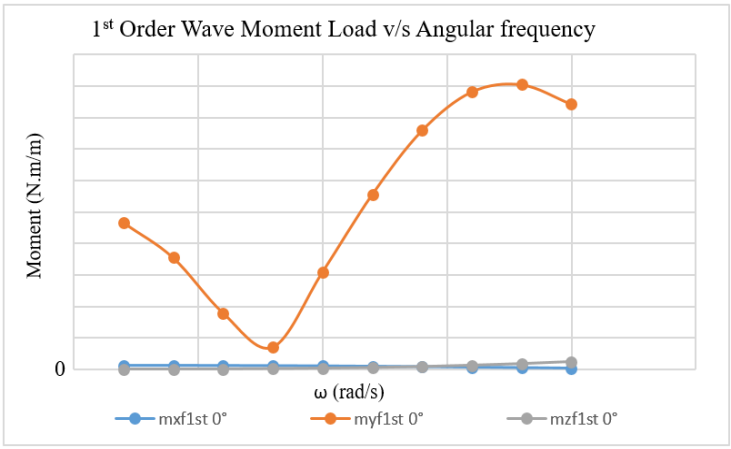

Figure 7-17. 1st Order Wave Moment Load

In Figure 7-18, the surge RAO is decreasing for low frequency range. This is because mooring stiffness decides the response in the surge direction. As the frequency increased, the surge response dipped until a frequency value and increased slightly afterward. The valley value of the frequency corresponds to the cancellation period of the platform, which is decided by the floater's hull shape.

Although the heave response is noticeable, the peak value is not excessive. This is due to the larger water plane area and the added mass due to heave. Furthermore, the peak value of the heave response is the platform's natural frequency. The response in sway motion is

zero as it is considered only in the 0º heading angle. The symmetrical nature of the platform also supports this.

Pitch RAO and heave RAO show similar behaviour because of pitch-heave coupling, as shown in Figure 7-19. The wavelength of most RAOs is significantly large at low frequencies, and the effect becomes more noticeable, adversely affecting the dynamic response of a platform.

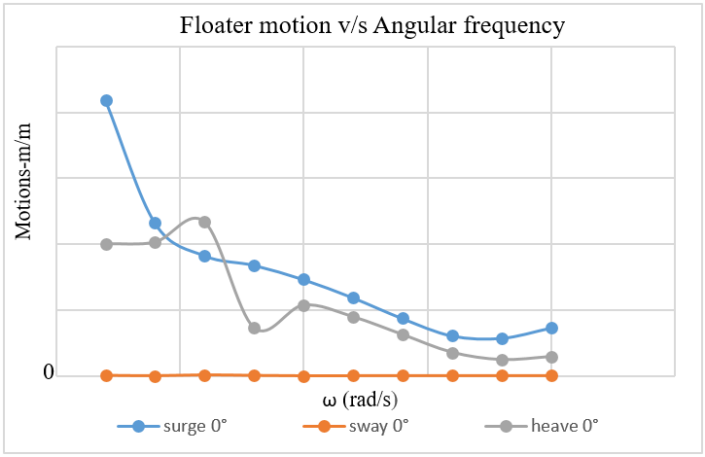

Figure 7-18. RAO of Surge, Sway, Heave

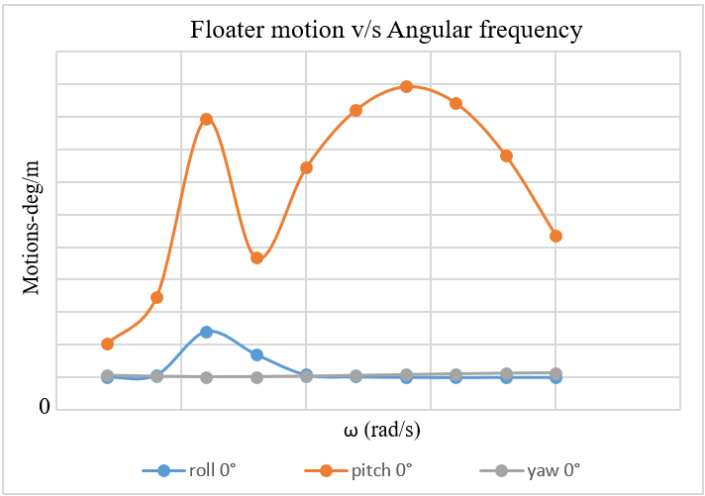

Figure 7-19. RAO of Roll, Pitch, Yaw

iii. 2nd Order Wave Load:

In this case, the wave load is expressed using Quadratic Transfer Functions (QTFs) of second order. Depending on the amplitude of the wave, these loads increase proportionally. Offshore platforms are subjected to significant slow-drift motions and ringing effects caused by second-order wave-excitation forces [13]. Based on the

interaction of two regular waves with frequencies ω_k and ω_l, low-frequency loads with a frequency of $|\omega_k - \omega_l|$ are generated. To model the low-frequency loads, one can define them as being a quadratic function of the bichromatic incident and diffraction/radiation wave fields [13]. By solving the second-order problem, the QTF of low-frequency loads can be obtained. QTF must be defined in an extensive frequency range in shallow water and digitized accurately [14]. This form is called Full QTF or QTFC.

It is necessary to evaluate the first-order wave field along the waterline and around the hull to formulate the near-field formulation. The offshore structure is taken as mesh, so the centre field formulation cannot work [13]. Thus, the near-field formulation is used in HydroStar. The complete QTF calculation requires the solution of the second-order potential. A complete QTF calculation has two steps: pre-processing by hsamg and calculation by hsqtf (low or difference of frequency) in HydroStar.

The drift loads result obtained from the HydroStar is shown below:

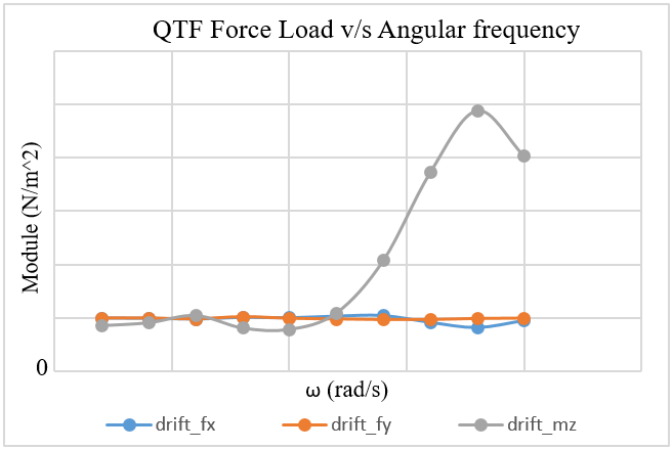

Figure 7-20. QTF Full Force load

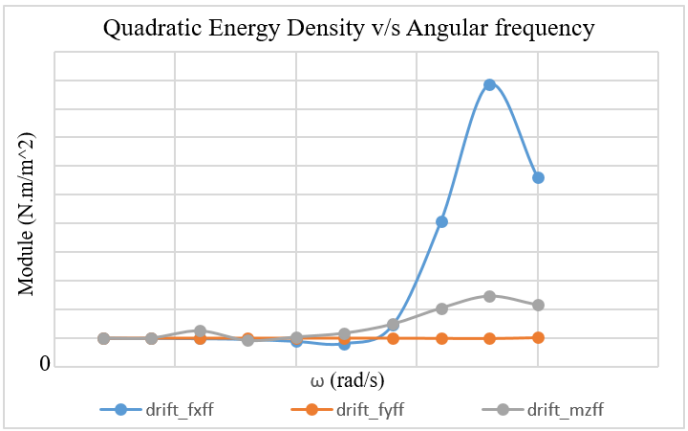

Figure 7-21. Quadratic Energy Density

Figure 7-20 and Figure 7-21 illustrate that the drift force and respective energy density are near zero for the small frequency value. It is due to low frequency; the floating structure is transparent to waves and does not diffract the wave and the drift force tends to zero. While at extremely high frequency, the structure behaves like a fixed breakwater, and thus the drift forces experienced are larger. Drift_mz is highest, showing that the second order wave forces are highest for heave direction.

7.1.2 Assembly of floater units

All the defined FOWT units are assembled using kinematic chain connections. Below is the kinematic chain of the assembled FOWT units:

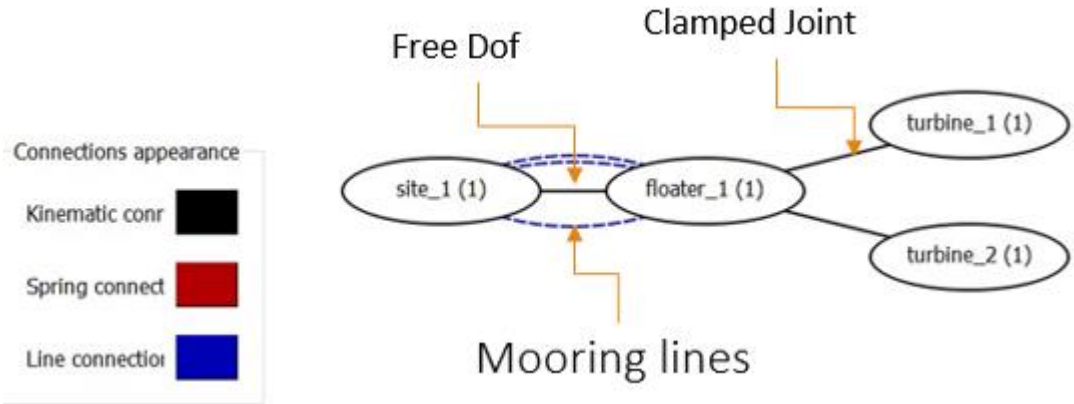

Figure 7-22. Kinematic Connection of FOWT units

From the above Figure 7-22, the following connection is developed:

1) The floater is connected to the seabed using mooring lines shown by blue dotted lines.
2) Floater relates to the seabed using kinematic connection with free DoF.
3) The other two turbine towers are clamped to their respective connection point on a floater.

7.1.3 Environmental loads

Different criteria's are presented in the BV standards to characterize the environmental conditions from which the loads should be calculated to determine structural response correspond to wind, marine, and aerodynamic effects [25]. The fatigue loads are usually found from the effect of "normal" environmental conditions that are likely to be exceeded at least once a year. Comparatively, the extreme conditions used for

defining the ultimate limit states refer to events likely to occur once every 50 or 100 years, depending on the specific standard or guideline [6].

Designing a FOWT must be structurally efficient, and characterization of the resulting load effects requires a sophisticated, detailed analysis of the specific conditions at a particular site. It is possible that the FOWTs within a wind farm site may be subject to different metocean conditions (i.e., meteorological, and oceanographic) and therefore requires distinctive designs.

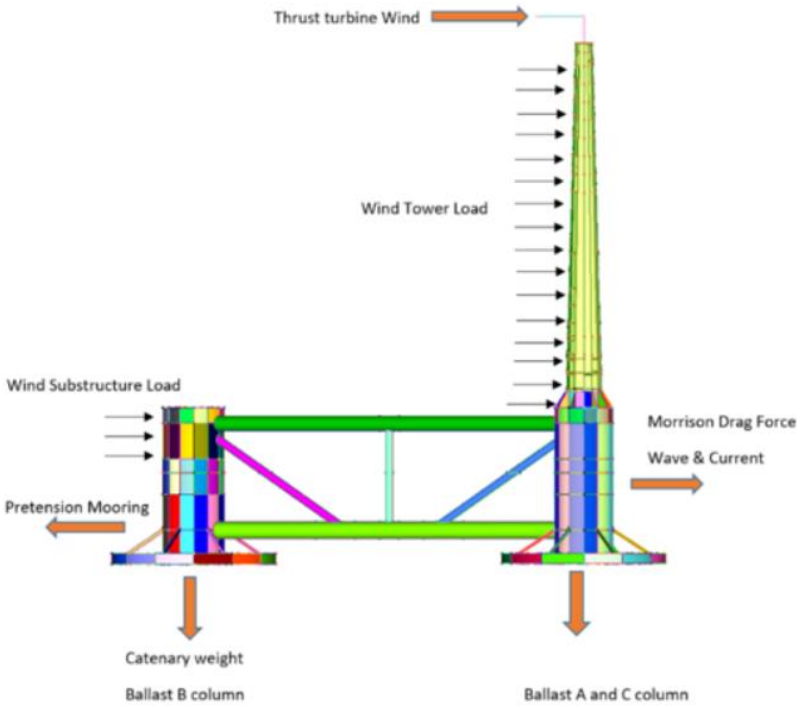

Figure 7-23. Loads showing in FOWT

Figure 7-23 shows the environmental loads acting on the FOWT's structure.

1) *Wind Load Cases:*

It is represented by the rotor's thrust and the tower's wind pressure. 61400-2, IEC's international standard, determines its value [6]. The thrust load is exerted on the point corresponding to the rotor as a punctual force (7.1). A pressure load is assigned to the wind pressure as a function of the tower height following the IEC standard [6]. In OPERA, the wind load is introduced as a pressure applied to the turbine tower and the platform area exposed to wind.

i. Thrust load:

The thrust load can be defined using the following formula for given environmental conditions:

a) Normal Operation Wind:

Wind turbines operate under this condition as part of their design [26]. Consequently, it is considered steady wind as the wind conditions are 'normal'. The thrust load in this condition is given by (7.1).

b) Parked Wind Load:

This condition refers to the parked case where the wind turbine blade is in IDLE condition. Thus, the projected area of the blade is considered to define the thrust force [23] as:

$$F=\frac{1}{2}\rho_{air}*V_{e50}^2*A_{proj,B}*N_B*C_D \tag{7.23}$$

Where, C_T=thrust coefficient with a value of 0.5,

C_D= the drag coefficient and shall be taken as 1.5,

N_B=number of blades-3,

$A_{proj,B}$=planform area of the blade-m^2,

This scenario analyses extreme conditions that are expected to be faced by the wind turbine.

ii. Pressure load:

Besides the thrust load and moment provided by the wind load, the turbine tower and exposed platform area are subjected to equivalent pressure load [23], which can be evaluated as:

$$P=0.5*\rho_{air}*C_D*V_a^2 \tag{7.24}$$

where,

P=equivalent pressure load-$\frac{N}{m^2}$,

V_a=wind intensity at the height z_a-$\frac{m}{s}$,

The intensity can be calculated using IEC 61400-2 as:

1. $V_a = V_{hub}\left(\frac{z_a}{z_{hub}}\right)^{0.2}$ for normal operating case,
2. $V_{e50} = 1.4 * V_{ref} * \left(\frac{z_a}{z_{hub}}\right)^{0.11}$ profile for extreme wind speed,

In OPERA, only the thrust load is imported to the hub, while the pressure force is calculated in the analysis using the data provided as wind time series same as Figure 7-7.

2) Wave Load Cases:

The applied wave load calculated with HydroStar for floater case is used in OPERA for the global structural response. The pressures calculated by the hydrodynamic solver are applied to the structural model. This load is assigned to the entire hull surface, showing the waterline (as well as the hydrostatic load). In this thesis, the Jonswap spectrum [20] is used to define the wave spectrum for the load as it is valid for wind sea to fully develop sea state for modelling wave loads.

$$S(f) = \alpha \frac{5}{16 f^5} \frac{H_s^2}{T_p^4} exp\left(\frac{5}{4 T_p^4 f^4}\right)^{\gamma^{exp\left(\frac{-\left(f-\frac{1}{T_p}\right)^2 T_p^2}{2\sigma^2}\right)}} \tag{7.25}$$

The parameter used to define this spectrum, significant wave height (H_s), peak period (T_p), and the Jonswap parameter γ, are provided by partners.

a) Normal wave condition:

It is the operating condition for which a wind turbine is designed. This type of loading case is cyclic and most often experienced by the turbine structure [23]. Supplied the data for H_s and T_p, the wave spectrum used in the OPERA analysis is given below:

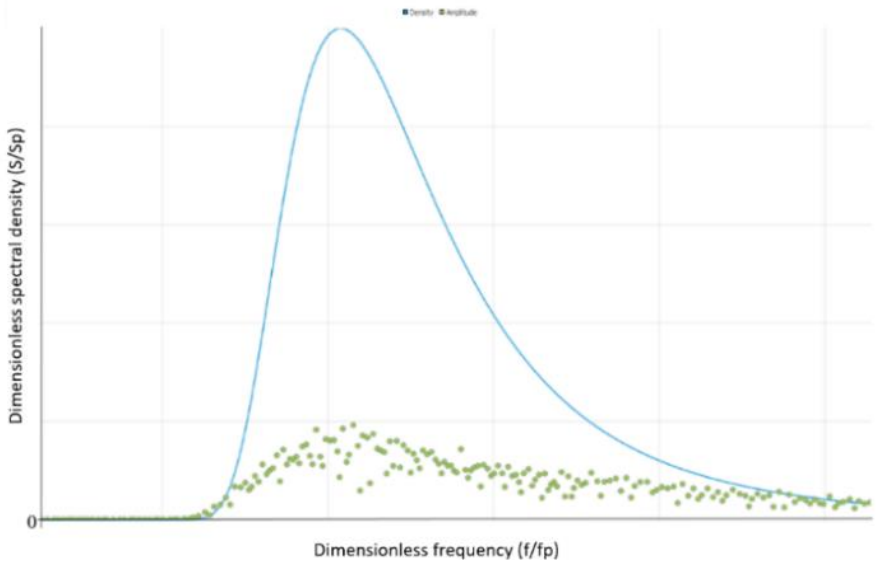

Figure 7-24. Jonswap Wave Spectrum (OPERA)

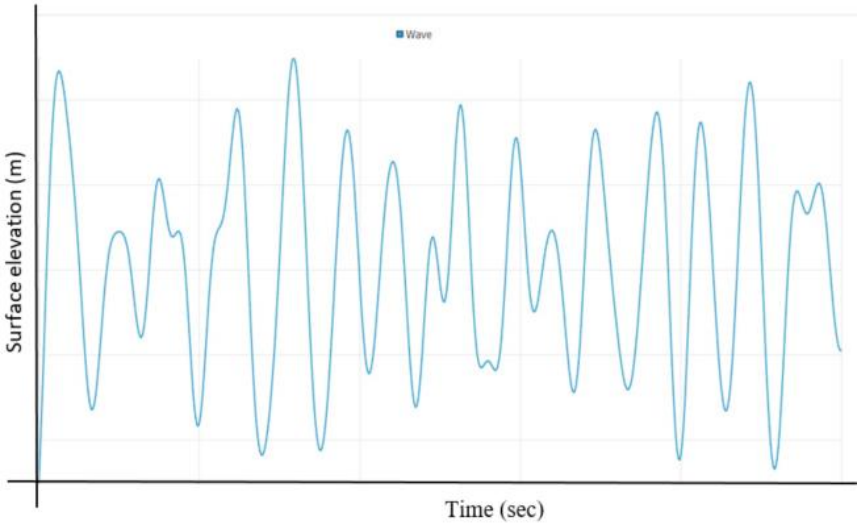

Figure 7-25. Time series Jonswap Spectrum

Production condition (Condition taken for Fatigue Analysis):

Table 7-4. Environmental parameter considered for production condition

Environmental Parameter	**Value**
Wave Spectrum	JONSWAP
Significant Wave Height	2.5 m
Peak Period	8.0 sec
Peak Enhancement Parameter (gamma)	1
Mean Wind speed	14.0 m/s
Heading angle	0º

7.1.4 OPERA Analysis

Figure 7-26 shows that the turbine tower is considered as rigid body followed by the aerodynamic coupling of turbine blades. These two elements are further discretized into the number of nodes to have a proper response spectrum in the load configuration section. The simulation is run for more than 10 minutes as per the DNV rule for a proper coupled analysis of floating wind turbines [27].

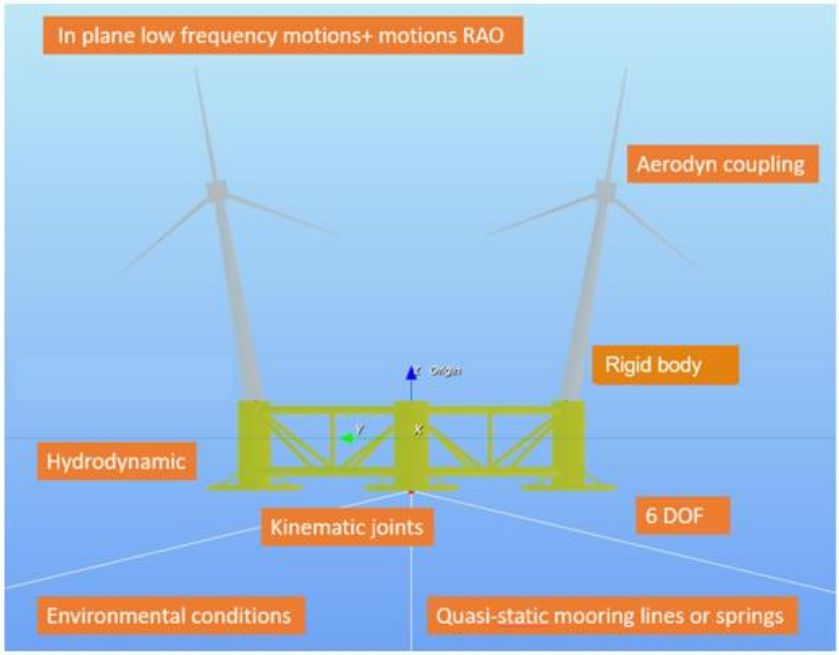

Figure 7-26. Analysis parameter consider in FOWT (OPERA)

In this analysis, the scheme used for the simulation is ERIK Dopri 5 mathematical integration algorithm. This is an explicit Runge-Kutta method of order 5 with step-size control and dense output [28]. It shows convergence for this FOWT structure, as shown in Appendix E. Figure 7-27, and Figure 7-28 illustrate the position of FOWT with time.

As FOWT interacts the wind load (shown as a green arrow in Figure 7-28) and the wave loads, the mooring lines show pretension load acting on it with the displacement in the positions. The floater draft is changing along the time act of load cases on it as shown in Figure 7-28.

The forces and moments load act on the FOWT structure are discussed in section 8.1. The stress in composite material in OPERA cannot be evaluated thus, the OPERA result is transferred to FEMAP, and further analysis is conducted.

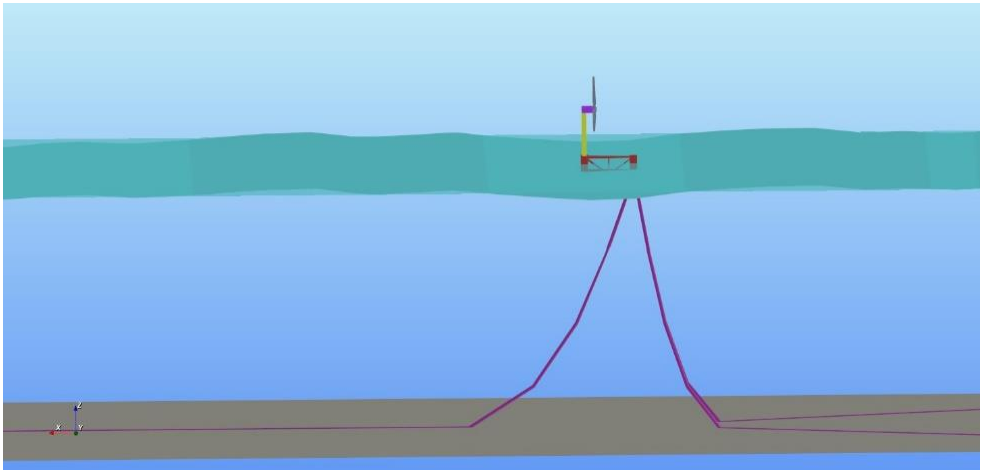

Figure 7-27. Position of FOWT at time 0 sec

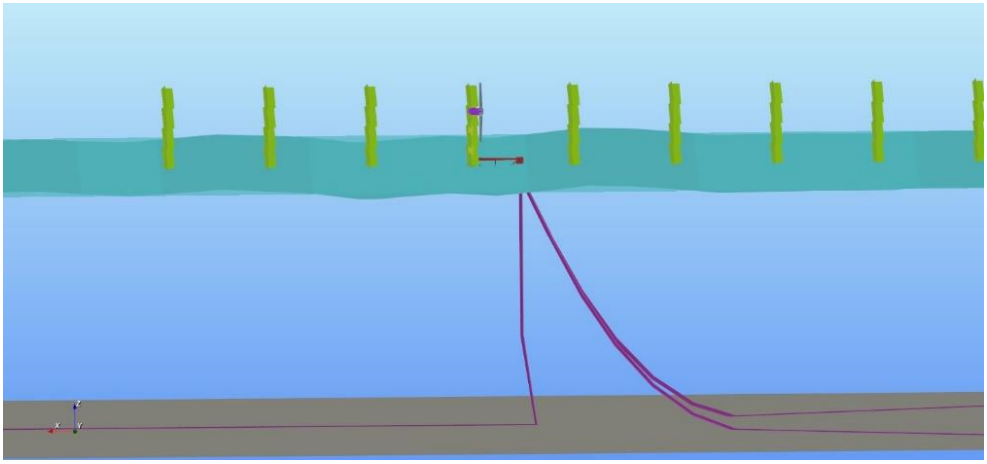

Figure 7-28. Position of FOWT at time 10 min

8 RESULTS AND DISCUSSIONS

8.1 Output of OPERA

After the successful compilation of the analysis, the output in OPERA is obtained as:

1. Moment Spectra
2. Force Spectra

The stress at each composite laminate is calculated for fatigue damage. The bottom of the tower base connection is considered as the most critical zone since larger bending moment occurs in this section due to large wind thrust.

8.1.1 Force load time series at the tower-base connection joint

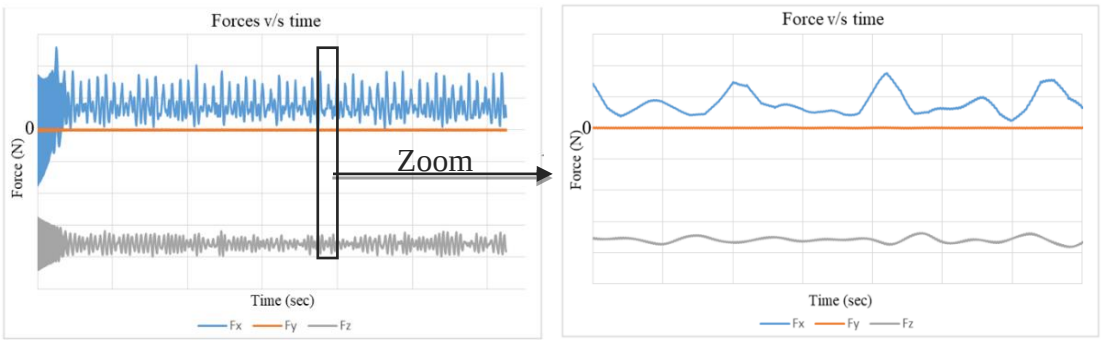

Figure 8-1. Force Load Time Series at Tower Base Joint (OPERA)

Oscillation can be seen in the first-time steps due to the inertia effects (Figure 8-1). It can be clearly seen that the forces in the wind direction (F_x), fluctuate in a similar way as that of rotor thrust load (Figure 7-8) with little increment due to the wind acceleration.

The force in the gravity direction (F_z) is simply the overall weight of the structure from the top of the tower to the base. The fluctuation in its value is supported by the effect of wave acceleration. Concerning the F_y, the force is negligible in comparison with the other two forces as the structure is heading to a 0°. The small value of (F_y)is due to the vector part of other forces as the tower is inclined. In the case of a straight turbine tower, the value in F_y should be equal to zero.

8.1.2 Moments load time series at tower-base connection joint

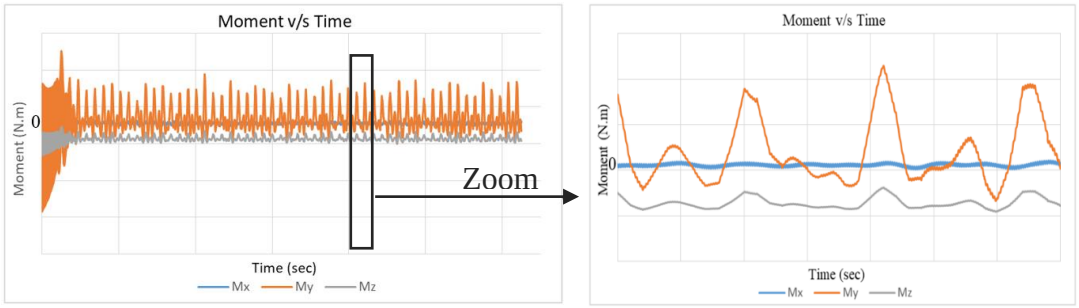

Figure 8-2. Moment Load Time Series at Tower Base Joint (OPERA)

Figure 8-2 illustrates the moment load time series at the tower base connection joints. The moment along the Y-direction (M_y) has larger effects than the other two moments. This is because the moment obtained from the applied thrust load plus the acceleration due to the waves. While the other moment, (M_z) is due to the waves and wind acceleration added by the gravity action. The moment (M_x) is due to the inclined nature of the tower, thus supported by the part of other moments.

8.2 Loads transfer from OPERA to FEMAP

The load generated by OPERA at the tower base connection is exported to FEMAP by transferring these loads to the hub point in FEMAP, keeping the same effect of force and moment at the tower base using a static equilibrium case.

$$\sum_{i=x,y,z} F_i = 0 \tag{8.1}$$

$$\sum_{i=x,y,z} M_i = 0 \tag{8.2}$$

The global axis in OPERA and FEMAP is not identical. So, the value on X-axis in Opera is on Y-axis in FEMAP, and the value on Y-axis in OPERA is on negative X-axis in FEMAP.

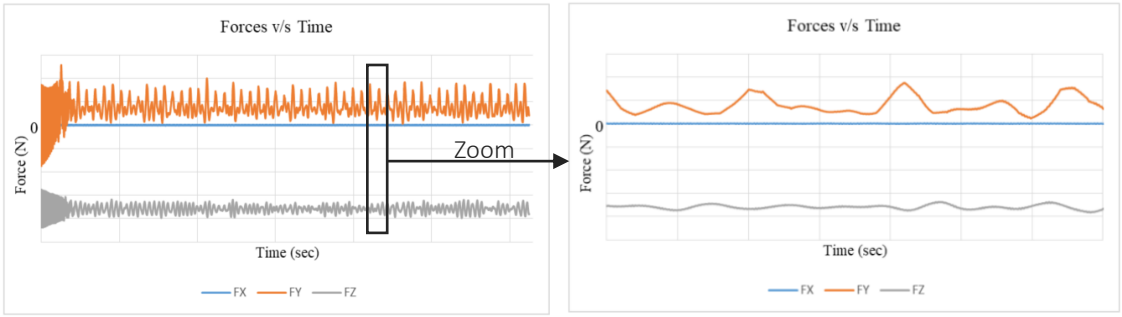

Figure 8-3. Force Load Time Series at Hub (FEMAP)

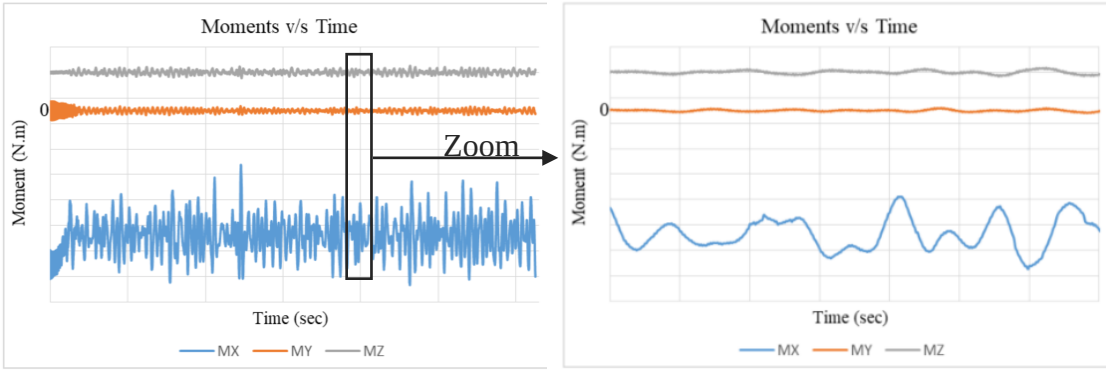

Figure 8-4. Moment Load Time Series at Hub (FEMAP)

As the load in Y-direction is more due to the wind rotor thrust, the moment defined by this load justifies the maximum moment observed in the X-direction, as shown in Figure 8-3, and Figure 8-4.

Further, the model and transient analysis of structure with dynamic loads are performed and discussed in next section.

8.3 Dynamic Analysis (FEMAP)

The time series of stress at each laminate is obtained from the transient load analysis. The most stressed laminates are considered critical and further processed to get fatigue damage life using Python script.

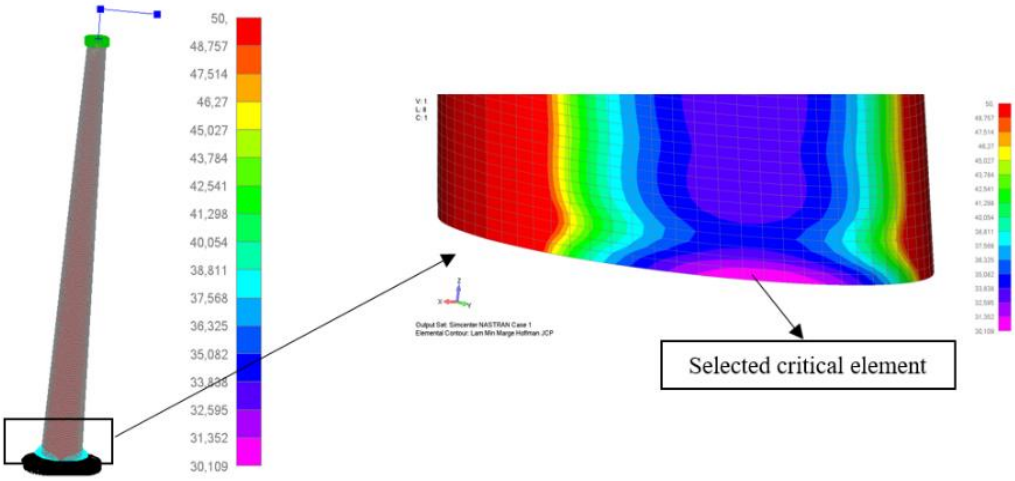

Figure 8-5. Critical Element Selected for Fatigue Methodology

Figure 8-5 illustrates the post processing data of FEMAP for the maximum hub load applied. The critical element is selected using minimum margin Hoffman criteria. This criterion defines the most critical element with margin value near to one. To perform fatigue analysis of complete structure, different elements are selected with higher Hoffmann margin value to perform the fatigue methodology in section 8.4.4.

Following the guidelines of fatigue methodology for composite materials derived by the Bureau Veritas for the calculations of fatigue life from section 4.1.1.1-4.1.1.6, a python script is written to analyse the material fatigue. After defining the critical elements, the static analysis for unit force and unit moment load is performed. The output obtained from FEMAP as X normal stress (σ_{11}), Y normal stress(σ_{22}), and XY Shear stress (σ_{12}) for all the plies of selected critical element is imported as CSV file to run in python Appendix G. This gives the fatigue damage values for each ply.

8.4 FATIGUE RESULT USING PYTHON SCRIPT

8.4.1 Rainflow Counting Algorithm

The stress obtained from the FEMAP is used to evaluate the equivalent fibre stress and equivalent matrix stress using (4.1) and (4.2) respectively.

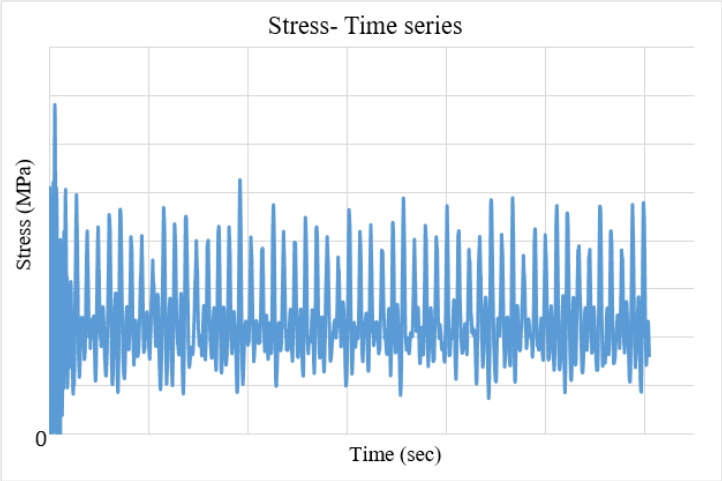

Figure 8-6. Stress-Time series for one ply of one element

Figure 8-6 illustrates the equivalent matrix stress-time series experience by one ply for given element. As seen from Figure 8-6, for different load applied to the structure, the stress experience by it varies. It results in alternative stress phenomena with both tensile and compression part.

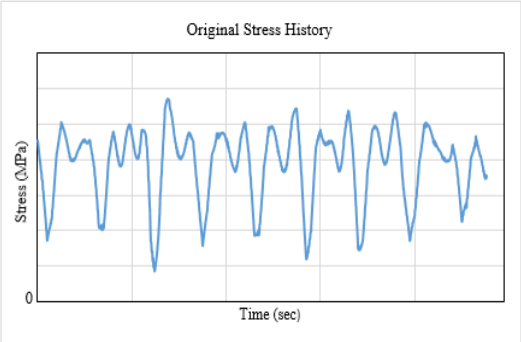

Figure 8-7. Stress-Time series for one ply for one element (Zoom-Section)

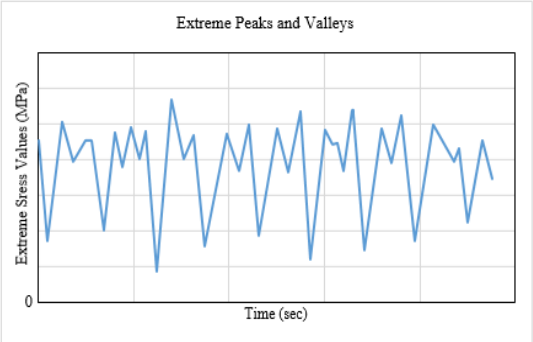

Figure 8-8. Extreme Peaks for stress using Rainflow

For each extreme of peak, the stress range is calculated using the maximum and minimum stress. Also, the stress ratio is calculated using (4.3).

Figure 8-9 illustrates the occurrence of the stress ratio value over time. For different stress ratio, the behaviour of composite material is different. Thus, it is essential to consider each stress ratio in the calculation and evaluate the total damage for each stress ratio for both fibre and matrix, respectively.

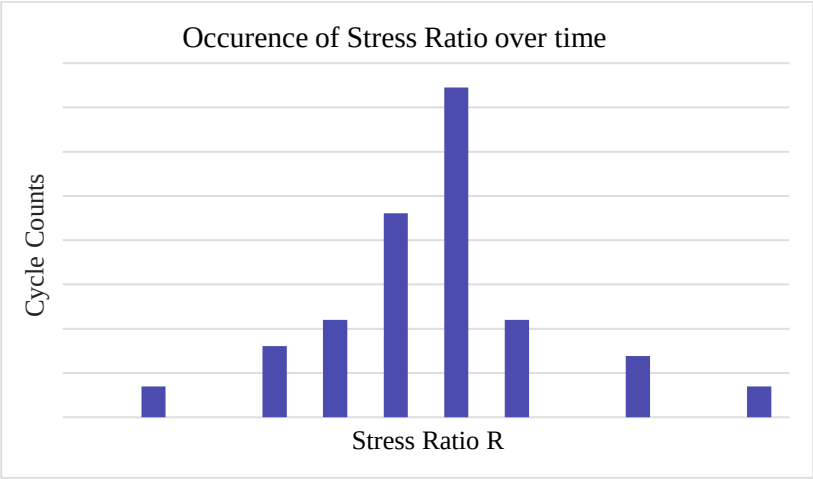

Figure 8-9. Variation in Stress Ratio R

Since, ply is experiencing alternative variable stress during its fatigue life. As per the BV guidelines, at least 3 *R* ratios are tested [10]:

1. *R*=0.1
2. *R*=10
3. $R=\sigma_{brc}/\sigma_{brt}$

These R values are selected considering tensile state at R=0.1 to compression state at R=10. These stress ratio R is used for CFL diagram.

8.4.2 SN Curve

The SN curve formulated based on the m coefficient (Table 4-1) for given stress ratio is as shown in Figure 8-10.

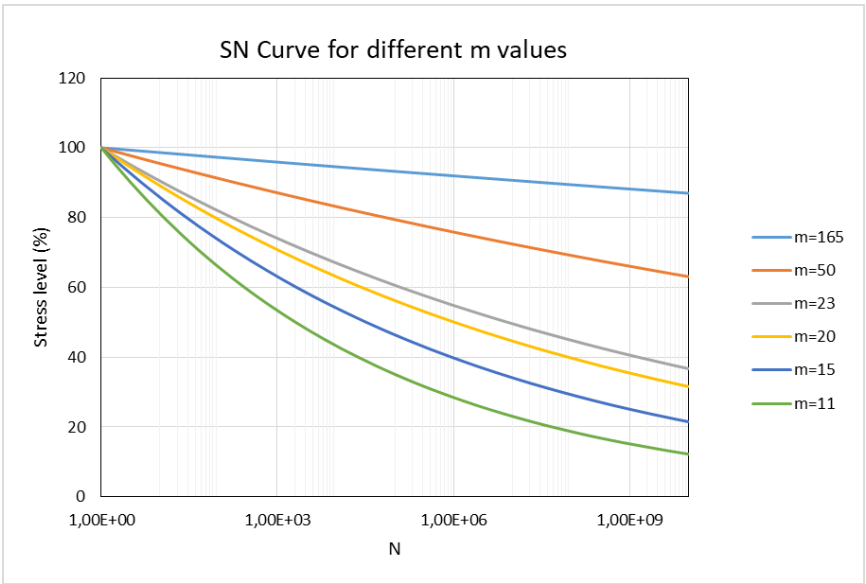

Figure 8-10. SN Curve for different m values

In Figure 8-10, the slope of SN curves is different for different m values, which also affect the damage value. The m coefficient value for carbon epoxy is large which reduces the slope (1/m) of given SN curve. For larger value of m, the SN curve is almost parallel to the horizontal axis. It means, either the stress needed to fatigue the given material needs to be large enough or the number of cycles of material before fatigue can be more. This concludes that larger the value of m, less is the chance of fatigue for the material. The SN curve obtained (Figure 8-10) is slightly small and has a minor damage value.

It can also be interpreted that the ply is experiencing different stress ratio other than R=0.1, R=-1, and R=10, so only SN curve is not sufficient to evaluate the total fatigue experience by the structure. To consider all the different stress ratios experienced by the ply in section 8.4.1, the CFL diagram has been translated into Python script using 4.1.1.4.

8.4.3 CFL Diagram

Figure 8-11 represent the CFL diagram for different stress ratio R. The maximum and minimum stress for a given stress ratio that the ply will sustain is calculated from (8.3), and (8.4) and using the python script.

$$\sigma_{max}=(\sigma_{mean}+\sigma_{alt})/2 \tag{8.3}$$

$$\sigma_{min}=(\sigma_{mean}-\sigma_{alt})/2 \tag{8.4}$$

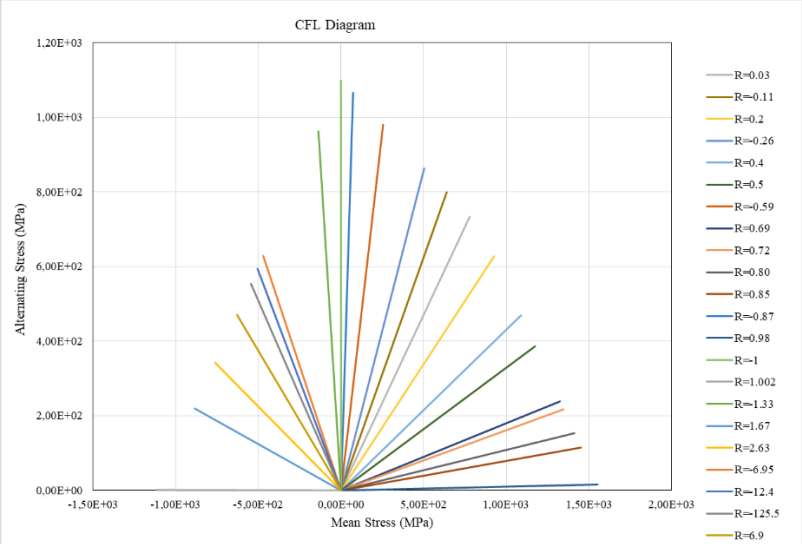

Figure 8-11. CFL Diagram for Different Stress Ratio R

The given ply is experiencing the tensile-tensile state as different R value is between 0-1. Less value of R is between to 1-10 showing that the compression state experiencing by this ply is not too much. Apart from that, the ply is experiencing all the four state such as tensile-tensile for R=0-1, tensile-compression state for R=0-(-1), compression-tensile state for R= (-1)-10 and the compression-compression state for R=1-10.

For all obtained stress ratio R, SN curve is obtained for calculated maximum stress (8.3). In Figure 8-12, SN curve is plotted for different R values.

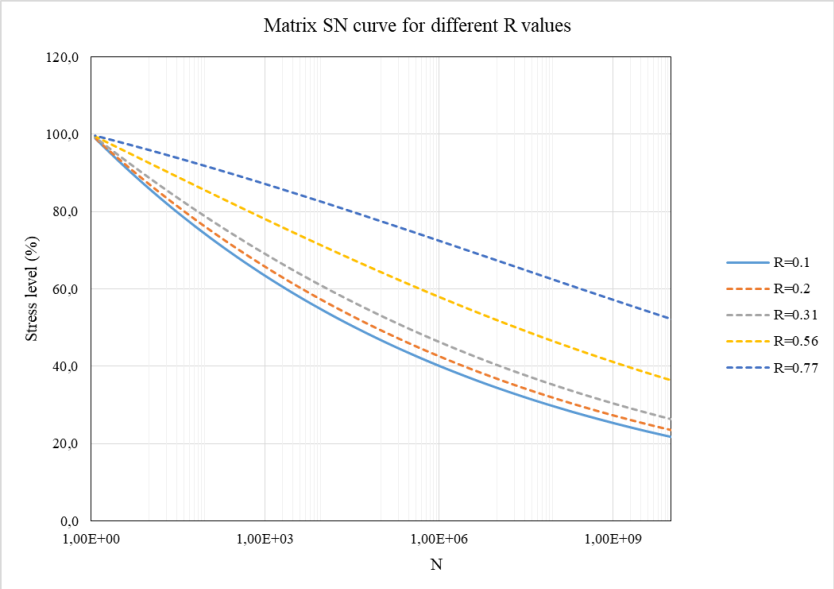

Figure 8-12. Goodman Analysis for SN Curve for different R values

It can be depicted from Figure 8-12 that for larger value of R, the SN curve is comparatively less slope than the smaller R values. This result in the requirement of larger stress load for failure of ply. This figure is used for the interpolation of SN data to eventually calculate damage values.

8.4.4 Damage Calculation

To show the methodology, linear-log curve for the SN diagram for stress ratio R=0.02 is plotted (Figure 8-13). For each R value, the number of cycles experienced by the ply is different.

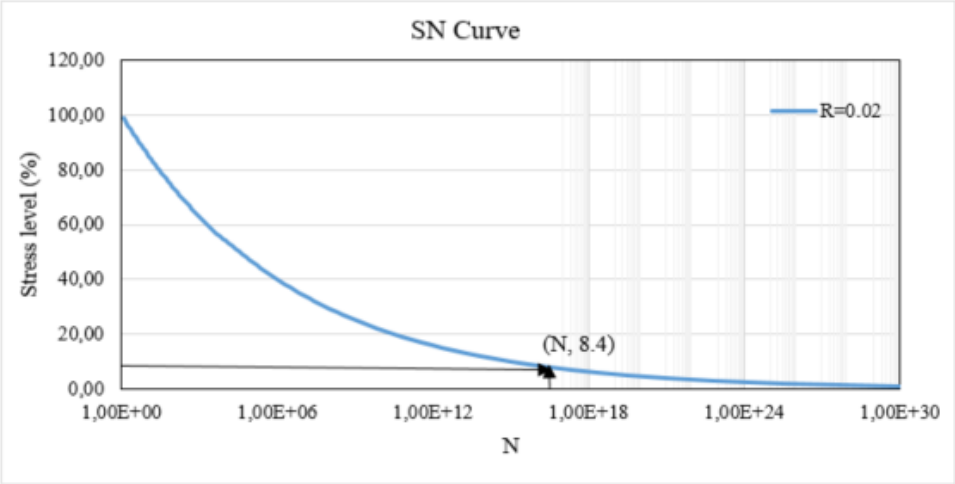

Figure 8-13. Use of SN Curve to find N for given stress

Therefore, using interpolation, the number of cycles to fatigue (N) for the given maximum stress is obtained. This process is performed for all R values to obtain different N cycles.

Considering the expected year of working of this FOWT is 20 years, the structural damage is evaluated using Miner's sum for all ply for a given element of both fibre and matrix using (4.8), and (4.9). The result obtained is shown in Table 8-1.

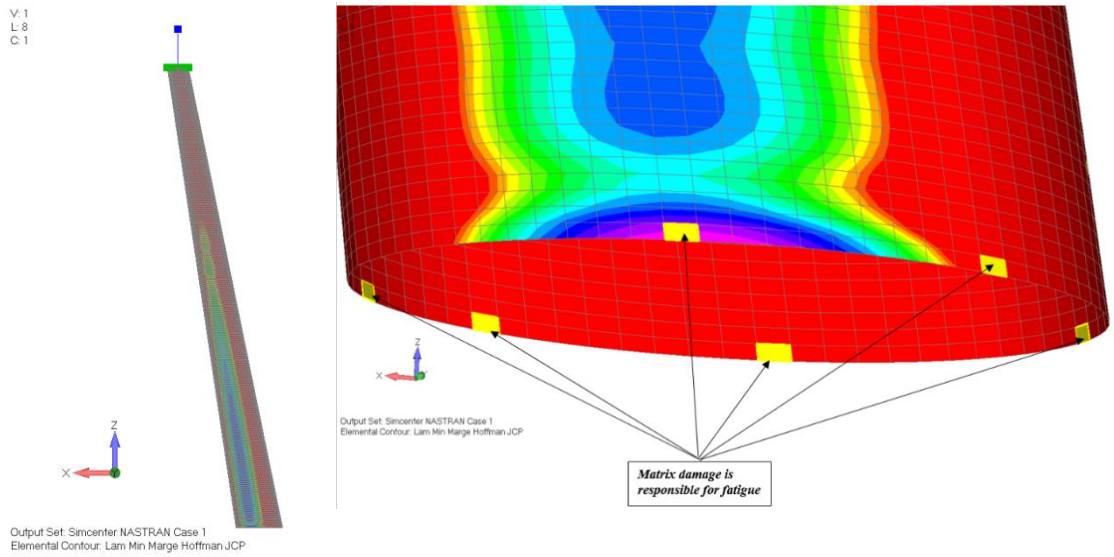

Figure 8-14. Damage in Critical Elements

Table 8-1. Total Damage of Selected Critical Elements

Element ID	Maximum Damage	Maximum Fibre Damage	Maximum Matrix Damage
282247	≈0	'Ply38': 2.71e-34	'Ply35': 3.66e-20
283777	≈0	'Ply38': 4.29e-26	'Ply32': 4.46e-19
286072	≈0	'Ply38': 1.87e-24	'Ply32': 1.36e-17
296211	≈0	'Ply38': 1.24e-63	'Ply32': 2.94e-47
299526	≈0	'Ply38': 9.33e-69	'Ply36': 4.28e-15
302076	≈0	'Ply38': 3.06e-62	'Ply36': 2.47e-13

The first three elements are in tensile state while the rest of three are in compression state. The fatigue phenomenon has less effect on the material in compression than in tension. It is concluded by the fatigue damage results of given elements. This is the case for each orientation, but it is even more pronounced at 45° and 90°. It seems that for those direction that are driven by the matrix behaviour, there is no influence of the compression on the fatigue life. Furthermore, transverse cracks and inter-laminar failure occurs in the matrix when given to tensile stress which leads to have more fatigue by matrix damage than that of fibre. So, all the elements shown in Figure 8-14 is prone to earlier matrix damage than to fibre.

The total damage is the maximum of fibre and matrix damage. As, the damage values is too small, it can be taken as zero. This zero-damage value result in longer lifetime of the FOWT structure as it is less prone to fatigue damage. Near zero value may have resulted from the fact that no safety factors or material ageing have been considered while evaluating damage. Also, the design is based on the static calculation in FEMAP, and large safety factors have been considered for this static calculation. Since the material used in carbon epoxy, the slope in SN curve is small and the stresses exerted by the plies for used loading condition is also small. This might result in near zero damage.

9 CONCLUSION

From this thesis, following conclusions can be formulated. To structure these conclusions, the outcome of each chapter along with the recommendations are discussed below.

9.1 Material Orientation (ComposeIT)

Using ComposeIT, the plies had been easily orientated in different directions for the laminates given the composite materials. But as discussed in 6.1, due to the actual limitation of this software, the safety factor of the composite material used in the scope of this thesis is yet to be defined.

9.2 Hydrodynamic Response of Floater (HydroStar)

For the designed platform, HydroStar successfully evaluated the hydrodynamic response on the platform for a given wind and wave loads. As the design is symmetrical and the heading angle is 0°, the first order wave loads in surge direction is calculated greater than the forces in other DoF. Similarly, due to the three heave plates attached to the columns, using the radiation/diffraction module of HydroStar, the added mass and the radiation damping for the heave motion are found to be larger.

HydroStar does not take the small braces into consideration assuming no more effect caused by these braces to the platform. The hydro mesh considered in HydroStar is also limited to less than ten thousand elements as per its actual limitation and time computation.

9.3 Global Structural Response on FOWT (OPERA)

OPERA software is still under development by the BV. The multiphysics knowledge like hydrodynamics, kinematic bodies, and aeroelasticity, used by this OPERA make it more prominent to be used in different fields and projects related to the marine and offshore. Using the time domain structural solver supported by the fifth order integration analysis scheme, the global structural response of FOWT due to environmental load is successfully analysed. The result would have been more realistic if the data related to the controller and blades were achieved prior to the thesis. Also, due to the actual limitation of OPERA, the flexible tower analysis is not possible yet. Following assumptions such as application of rotor hub load directly instead of controller,

rigid body analysis of tower instead of flexible, assumed value of damping loads, and the blade data values are taken into consideration while performing this thesis. Thus, the result might deviate from its realistic nature.

9.4 Fatigue Methodology used in Python

The methodology introduced in this thesis shows how fatigue life can be assessed with the damage accumulation based on the SN curve and the CFL diagram. The graphical analysis of the damage value results shows that different environmental factors affect the fatigue life of FOWT. The most critical load cases are the wind loads in connection with wind direction and connected to the thrust load, which was discussed in the OPERA section. Compared to the fatigue study in metals, there is still more to learn and discover about the fatiguing nature of composite materials. The Composite material section of Bureau Veritas Marine & Offshore has consistently developed the fatigue methodology for the composite materials. This process is ever evolving based on the research data available on this subject. To date, the fatigue methodology developed for composite materials illustrates no fatigue damage in the turbine tower made up of composite materials because no safety factor has been considered yet. On applying the safety coefficient, the stress, loads, and damage value will deviate by a small margin which will be the future work on this thesis topic. Thus, for the first model case, the plies for the tower made of carbon epoxy respect the design life of 20 years with almost negligible damage value.

REFERENCES

[1] Enerocean, "SAR-- - Structural Analysis Report - Rev 0-BV.pdf," 2021.

[2] BMT FLEET TECHNOLOGY LIMITED, "FATIGUE DESIGN REVIEW OF OFFSHORE WIND TURBINE GENERATOR STRUCTURES," United States Department of the Interior Bureau of Safety and Environmental Enforcement,, 2013.

[3] COMPASSIS, "DESIGN_BASIS_DRAFT_APPROVAL_IN_PRINCIPLE_V4.pdf," 2022.

[4] G. Meryem, "Fatigue analysis of a tidal turbine blade in composite material.," Master degree, UPM, 2021.

[5] J.García-Espinosa. An Introduction to FIBREGY project [Online] Available: https://www.scipedia.com/public/Draft_Garcia-Espinosa

[6] I. E. Kommission, "Design requirements for floating offshore wind turbines," 2019.

[7] H. S. Kim and S. Huang, "S-N Curve Characterisation for Composite Materials and Prediction of Remaining Fatigue Life Using Damage Function," *Journal of Composites Science*, vol. 5, no. 3, 2021, doi: 10.3390/jcs5030076.

[8] B. Dale, "Fatigue Design Review of Offshore Wind Turbine Generator Structures," United States Department of the Interior Bureau of Safety and Environmental Enforcement, 2013.

[9] B. Li, K. Rong, H. Cheng, Y. Wu, and P. Wang, "Fatigue Assessment of Monopile Supported Offshore Wind Turbine under Non-Gaussian Wind Field," *Shock and Vibration*, vol. 2021, pp. 1-12, 2021, doi: 10.1155/2021/6467617.

[10] B. V. C. M. Section, *Composite fatigue Guidelines_v0.2*. B. V. Marine & Offshore, 2022.

[11] S. D. I. Software, "FEMAP," ed, 2022.

[12] B. V. M. Offshore, *COMPOSEIT SOFTWARE DESIGN ASSESSMENT OF COMPOSITE SHIP STRUCTURE*. B. V. Marine & Offshore, 2022.

[13] B. V. M. Offshore, *HydroStar*. B. V. Marine & Offshore, 2022.

[14] B. V. M. Offshore, *OPERA Software*. B. V. Marine & Offshore, 2022.

[15] B. V. C. M. Section, *Hull in composite materials and plywood, material approval, design principles, construction and survey*. B. V. Marine & Offshore, 2020.

[16] B. K. Lee and J. K. Lee, "Buckling of Tapered Heavy Columns with Constant Volume," *Mathematics*, vol. 9, no. 6, 2021, doi: 10.3390/math9060657.

[17] I. N. M. Kawai, "A failure-mode based an isomorphic constant life diagram for a unidirectional carbon/epoxy laminate under off-axis fatigue loading at room temperature," 2013. [Online]. Available: https://journals.sagepub.com/doi/10.1177/0021998313476324.

[18] A. G. a. K. K. Singh, "Fatigue behavior of FRP composites and CNT-Embedded FRP composites: A review: Fatigue Behavior of FRP Composites and CNT-Embedded FRP Composites," *Polym. Compos*, vol. 39, pp. 1785–1808, 2018, doi: 10.1002/pc.24177.

[19] K. K. a. C. Ad, "Load Ratio Effect on the Fatigue Behaviour of Adhesively Bonded Joints: An Enhanced Damage Model," p. 26.

[20] H.-J. M. S. Bungartz, "Fluid-structure Interaction: Modelling, Simulation, Optimization," *Springer-Verlag*, 2006.

[21] D. W. I. Association. "The Electronic Wind Turbine Controller." http://xn--drmstrre-64ad.dk/wp-content/wind/miller/windpower%20web/en/tour/wtrb/control.htm#:~:text=The%20wind%20turbine%20controller%20consists,motors%20within%20the%20wind%20turbine (accessed).

[22] O. Ray, "Pitch Control Critical for Wind Power," 2018. [Online]. Available: https://www.machinedesign.com/mechanical-motion-systems/article/21836463/pitch-control-critical-for-wind-power.

[23] B. V. M. Offshore, *Current and Tidal Turbine*. B. V. Marine & Offshore, 2015.

[24] M. N. M. K. Al-Solihat, "Mooring and Hydrostatic Restoring of Offshore Floating Wind Turbine Platforms," *Research Gate*, 2020. [Online]. Available: https://www.researchgate.net/publication/282220770.

[25] S. O. S. Bashetty, "Review on Dynamics of Offshore Floating Wind Turbine Platforms," 2021. [Online]. Available: https://www.mdpi.com/1996-1073/14/19/6026/htm.

[26] B. V. M. Offshore, *Classification and Certification of Floating Offshore Wind Turbines*. B. V. Marine & Offshore, 2019.

[27] DNV, *Coupled analysis of floating wind turbines* (R.-0286 DNV). 2021.

[28] E. H. a. G. Wanner. "Erik Dopri 5." Universite de Geneve. https://docs.scipy.org/doc/scipy/reference/generated/scipy.integrate.ode.html (accessed).

APPENDIX

Appendix A

Mesh Convergence of Tower

Figure A 0-1. Mesh size 200 mm

Figure A 0-2. Mesh size 20 mm

Modal Analysis	Frequency (Hz)
Mode 1	19.12
Mode 2	25.14
Mode 3	43.66
Mode 4	49.90
Mode 5	62.99

Modal Analysis	Frequency (Hz)
Mode 1	2.25
Mode 2	2.29
Mode 3	10.58
Mode 4	26.63
Mode 5	39.59

Appendix B

Modal Analysis

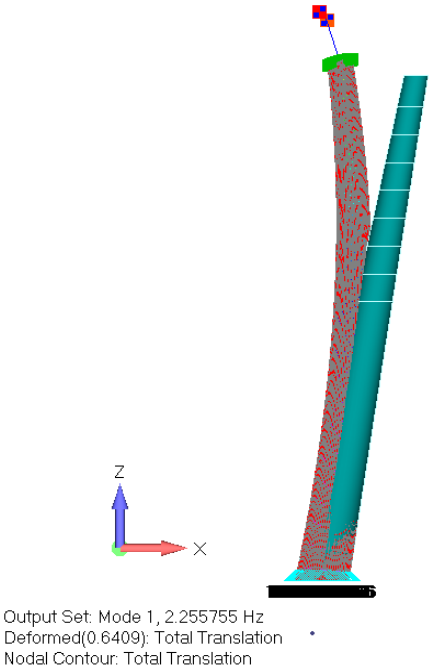

Figure A-0-4. Bending in X-axis

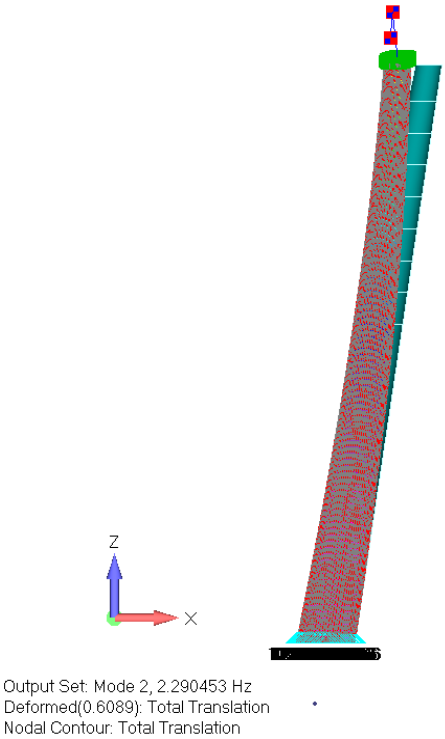

Figure A-0-3. Bending in Y-axis

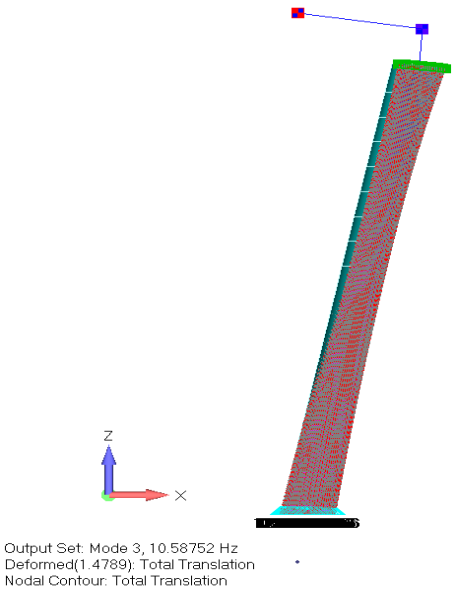

Figure A-0-5. Torsion along Z-axis

Appendix C

HydroStar

In this project, the following HydroStar Structure are used:

Hslec: Reading the mesh

Input: Body's geometry (coordinates, panel connectivity, and condition of symmetry)

Output: Hydrostatic properties of the body (Volume, centre of buoyancy, wetted surface, water plane area and inertia, etc).

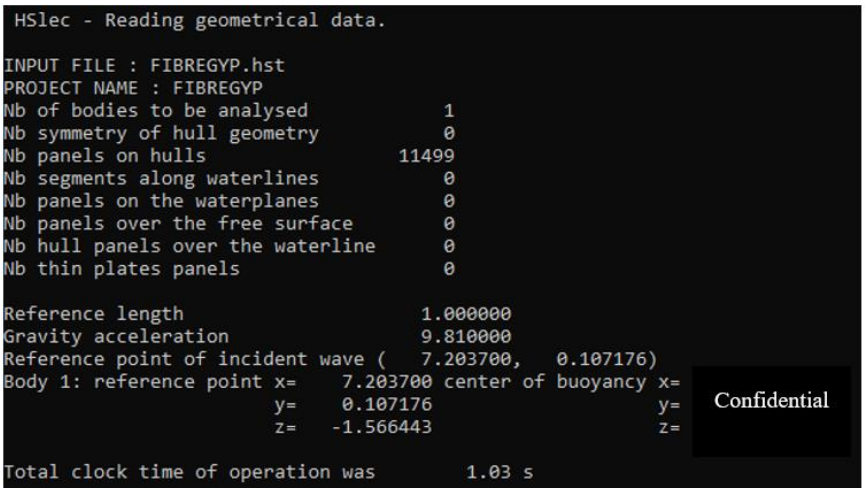

Figure A-0-6. Hydrostatic Properties of body

Hschk: Verification of the mesh

Input: Output of hslec

Output: Check of mesh (inconsistency, normal orientation, etc).

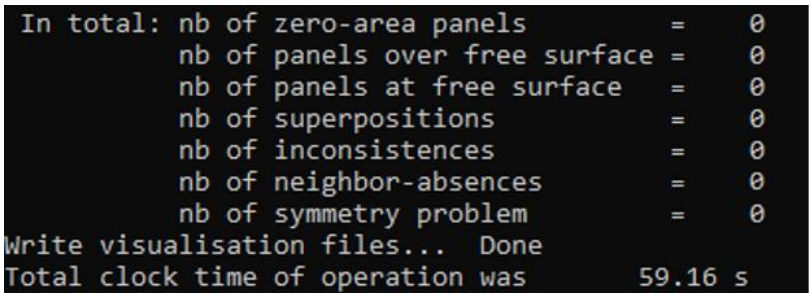

Figure A-0-7. Verification of Mesh in HydroStar

Hvisu: Visualization of the mesh

Input: Output of Hschk

Output: View of the mesh

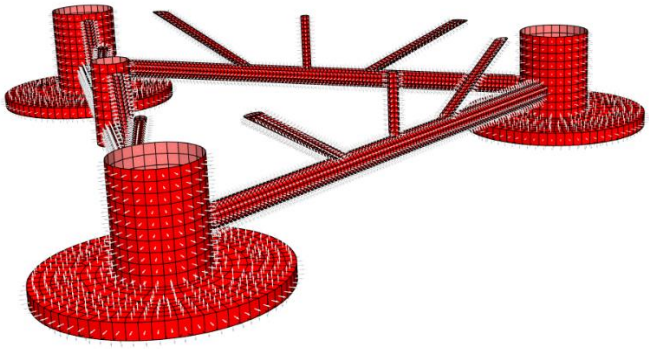

Figure A-0-8. View mesh in HydroStar

Hsrdf: Radiation and diffraction computation

Input: Wave conditions (wave frequencies and headings, water depth)

```
FILENAME platform

FREQUENCY TYPE  2
WMIN    0.1
WMAX    2.0
WSTP    0.1
ENDFREQUENCY

HEADINGS        TYPE    1
0.0     30.0    45.0    60.0    90.0    135.0   150.0   180.0   210.0   245.0   270.0   310.0   345.0   360.0
ENDHEADINGS

#SPEEDS TYPE    0
#1      0.0
#ENDSPEEDS

WATERDEPTH      CONFIDENTIAL.

ENDFILE
```

Figure A-0-9. Input File for radiation/diffraction in HydroStar

Output: Elementary solutions including added mass, radiation damping, and wave excitation loads

Hsmcn: Motions computation

Input: Mechanic properties (mass distribution, added stiffness, and added damping matrices)

Output: Motions of floating bodies

Hsamg: Pre-processing for second-order low-frequency computation in unidirectional and bi-directional waves

Input: Choice of formulation type (near filed or middle field); difference-frequencies and wave frequencies for the computation

```
DIFFREQUENCE    0.0     0.1     0.1
WAVFREQUENCE    0.1     2.0     0.1
TYPEFORMULE     NEAR-FIELD

ENDFILE
```

Figure A-0-10. Input file for hsamg

Output: Input files for hsqtf

Hsqtf: Second-order low-frequency computation in unidirectional or bi-directional waves

Input: Same as hsamg

Output: Second-order low-frequency loads in unidirectional and bi-directional waves

Hsdft: Second-order drift computation in unidirectional wave

Input: Choice of formulation type (near-field)

Output: Second-order drift loads in unidirectional waves

Hsrao: Construction of the transfer function

Input: Choice of which transfer function the users want to construct and the name of the file to store the results

Output: Transfer functions of motions, velocities, accelerations, and second-order loads.

```
CM      FILE    adm.dat TERM    11      22      33      44      55      66
CA      FILE    dmp.dat TERM    11      22      33      44      55      66

GSURGE  BODY    1       FILE    surge.rao       AMP
GSWAY   BODY    1       FILE    sway.rao        AMP
GHEAVE  BODY    1       FILE    heave.rao       AMP
GROLL   BODY    1       FILE    roll.rao        AMP
GPITCH  BODY    1       FILE    pitch.rao       AMP
GYAW    BODY    1       FILE    yaw.rao AMP

FXF1ST  FILE    fxf1st.rao      AMP
FYF1ST  FILE    fyf1st.rao      AMP
FZF1ST  FILE    fzf1st.rao      AMP
MXF1ST  FILE    mxf1st.rao      AMP
MYF1ST  FILE    myf1st.rao      AMP
MZF1ST  FILE    mzf1st.rao      AMP

DRIFTFX BODY    1       FILE    drift_fx.qtf    PRE
DRIFTFY BODY    1       FILE    drift_fy.qtf    PRE
DRIFTMZ BODY    1       FILE    drift_mz.qtf    PRE
DRIFTFX BODY    1       FILE    drift_fxff.qtf  MOM
DRIFTFY BODY    1       FILE    drift_fyff.qtf  MOM
DRIFTMZ BODY    1       FILE    drift_mzff.qtf  MOM
```

Figure A-0-11. Output Requested by Hsrao

Appendix D

Static Analysis

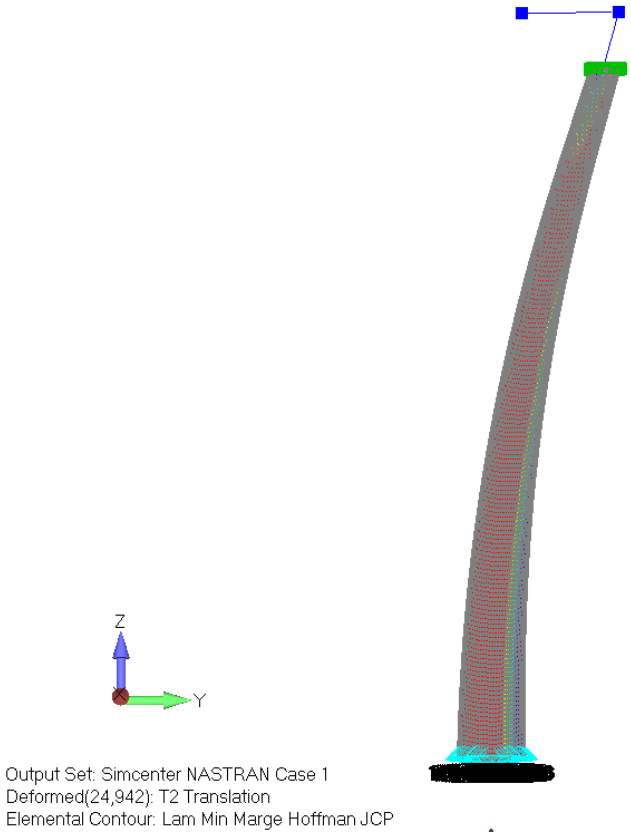

Figure A-0-12. Maximum Load Applied (Force+ Moment) for Static Analysis

Appendix E

Selection of Analysis Scheme in OPERA

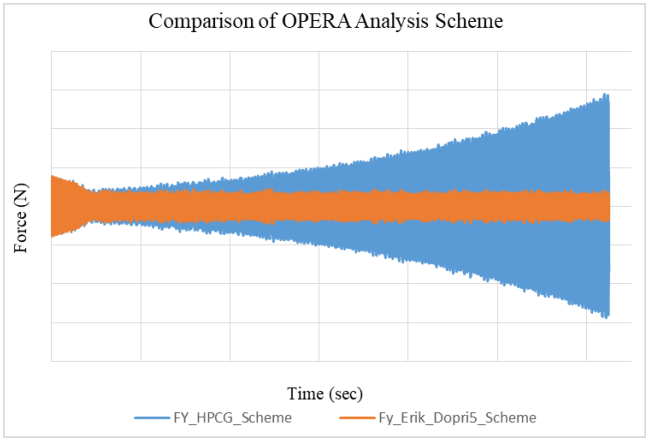

Figure A-0-13. Comparison of Analysis Scheme in OPERA

Appendix F

Comparison of Opera Analysis with load cases

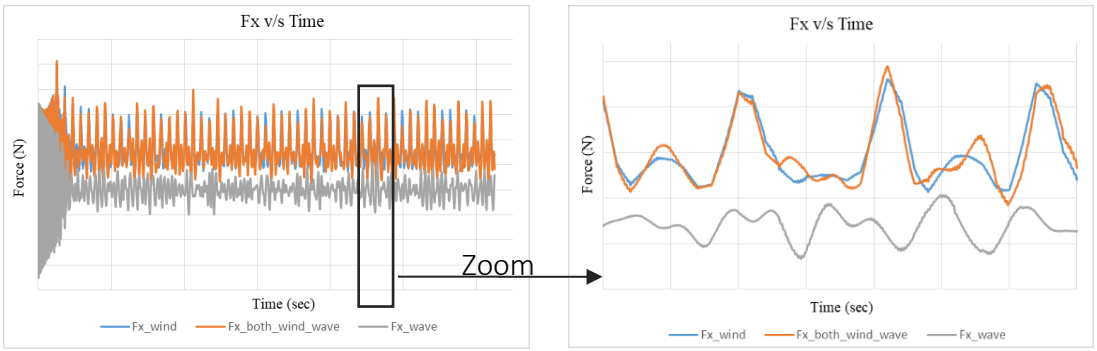

Figure A-0-14. Fx time series for wind, wave, and wind-wave loading cases.

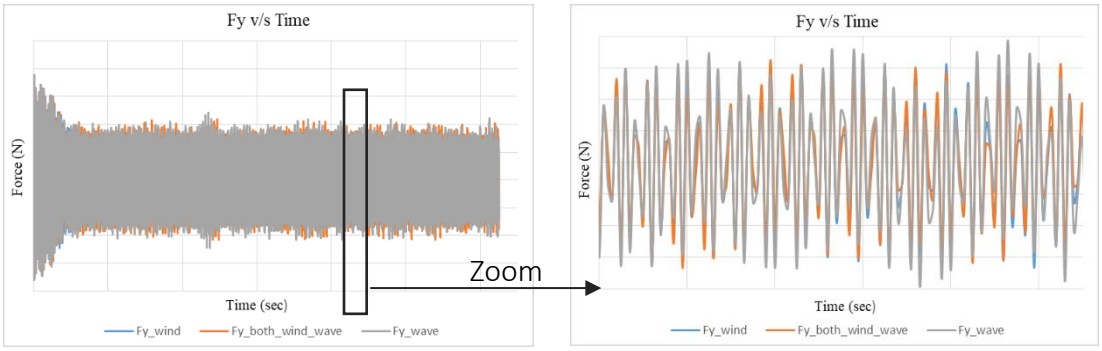

Figure A-0-15. Fy time series for wind, wave, and wind-wave loading cases.

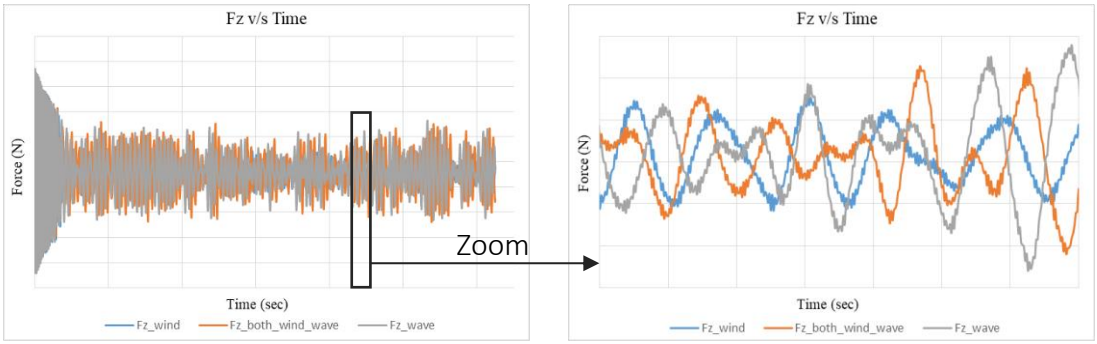

Figure A-0-16. Fz time series for wind, wave, and wind-wave loading cases.

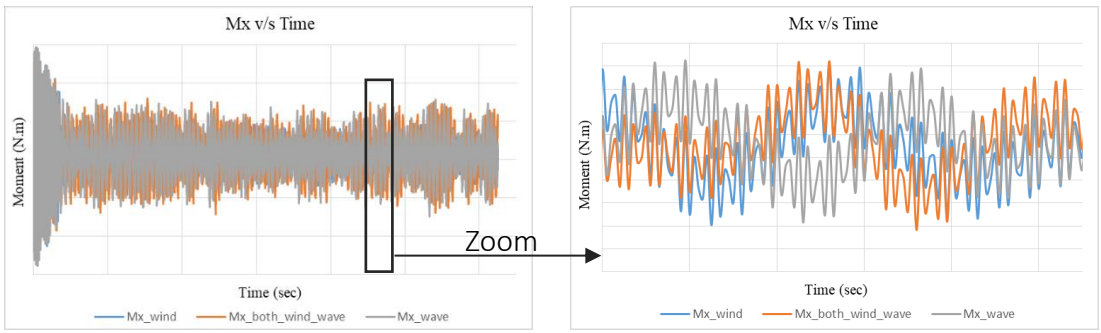

Figure A-0-17. Mx time series for wind, wave, and wind-wave loading cases.

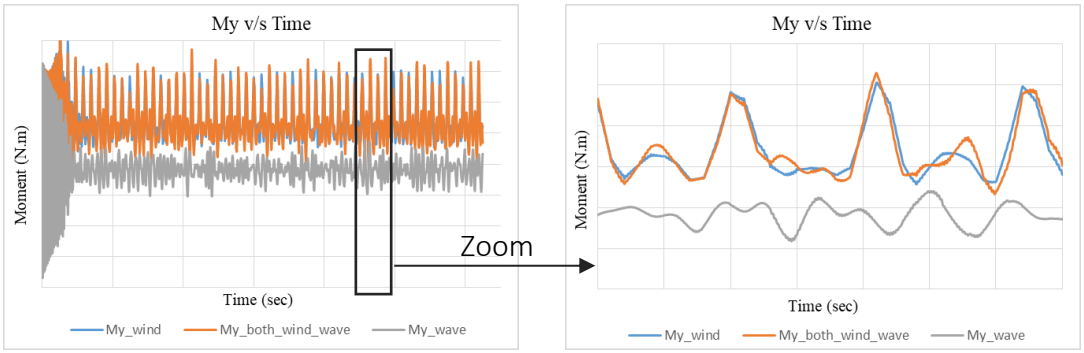

Figure A-0-18. My time series for wind, wave, and wind-wave loading cases.

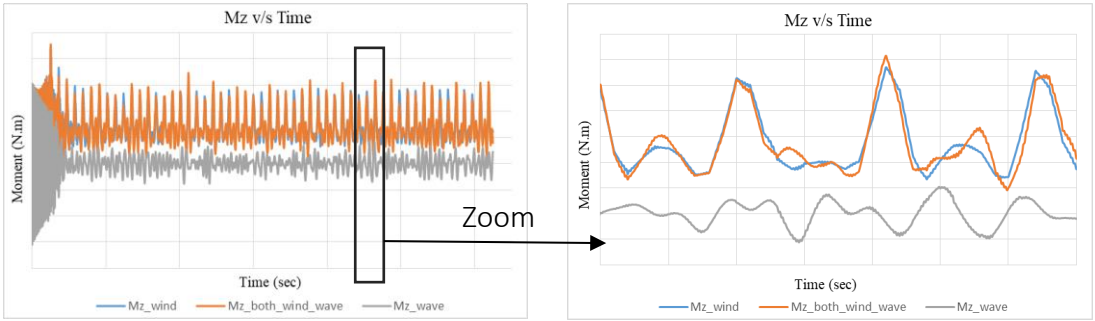

Figure A-0-19. Mz time series for wind, wave, and wind-wave loading cases.

Appendix G

Python Script

filterDataByXY.py

```
# Function defines to filter the stress data as X Normal stress, Y Normal Stress, and XY Normal Stress
def filterDataByXY (filepath, n_laminate):
  result= []
  array= []
  dataset=pd. read_csv(filepath)
  for i in range (1, n_laminate+1):
    colunmar_data_based_filter_list=[f.” *Ply{i} X Normal Stress",f".*Ply{i} Y Normal Stress",f".*Ply{i} XY Shear Stress"]
    for filter_items in colunmar_data_based_filter_list:
        converted_dataset=dataset.columns.values.tolist()
        r = re.compile(filter_items)
        filtered_list = list(filter(r.match, converted_dataset))
        result.append(filtered_list)
    array.append(result)
    result=[]

  return array, dataset

def XYDataSeparation(array, dataset):
  X=None;
  Y=None;
  XY=None;
  data_fibre=[]
  data_Y=[]
  data_XY=[]

  for idx, i in enumerate(array):
     for idx, i in enumerate(array[idx]):
        if idx==0:
           X=dataset[i]
           data_fibre.append(X)

        if idx==1:
           Y=dataset[i]
           data_Y.append(Y)
        if idx==2:
           XY=dataset[i]
           data_XY.append(XY)

  return data_fibre, data_Y, data_XY

def cleanAndFilteredData(filepath,n_laminate):
  filterData=filterDataByXY(filepath,n_laminate)
  dataSeparator=XYDataSeparation(filterData[0],filterData[1])
  return dataSeparator, filterData[1]
```

main.py

```
import numpy as np
import pandas as pd
import rainflow
import math
from scipy.interpolate import interp1d

# Loading CSV file for laminate stress
filepath=r"C:\Users\phpathak\OneDrive-
BureauVeritas\Bureau\Fibregyreportbyme\Python\raw_data302076.csv"

# Loading material data for each ply
material_data=pd.read_csv(r"C:\Users\phpathak\OneDrive-
BureauVeritas\Bureau\Fibregyreportbyme\Python\Fibregy\results_elem 302076.csv")

# Number of plies for given composite laminate
n_laminate = 38
# Tensile stress for fibre
sigmabrtf = material_data.iloc[:,1]
# Compressive stress for fibre
sigmabrcf = -material_data.iloc[:,2]
# Tensile stress for matrix
sigmabrtm = material_data.iloc[:,3]
# Compressive stress for matrix
sigmabrcm = -material_data.iloc[:,4]
# Shear stress for matrix
tau = material_data.iloc[:,5]
# m coefficient for fibre taken for SN curve of composite from Composite Guideline from BV
m1_f= [23,20, 50]
# m coefficient for fibre taken for SN curve of composite from Composite Guideline from BV
m1_m=[11,15,165]
# ratio of theoretical stress to maximum stress used for SN curve diagram
sigma_i1 = np.arange(0.00001, 100.001, 1)
# number of cycle to fatigue for 20 years n=20*365*24*60*60/600, the time duration is 605 sec in consideration
for transient
nb_cycle_fatigue = 1042512
# stress ratio available for CFL diagram analysis
R1 = [-1, 0.1, 10]
# defining alternate stress ratio for given R
p1_value = []
for R in R1:
    p_1 = (1 + R) / (1 - R)
    p1_value.append(p_1)

# Importing function to filter the given data in X, Y and XY
from filterXY import cleanAndFilteredData
dataSeparator, dataset = cleanAndFilteredData(filepath, n_laminate)
data_fibre = dataSeparator[0]
data_Y=dataSeparator[1]
data_XY=dataSeparator[2]

# Function considering the work for fibre
def fibre(n_laminate,data_fibre,sigmabrtf ,sigmabrcf):
  plycollection_fibre=[]
  damage_collection_fibre=[]
  collection_damage_fibre_value=[]
```

```
# loop for use of all plies
  for i in range(0, n_laminate):
      data_new = data_fibre[i].T.squeeze()
# importing the commmon part of formula for fibre
      result_value = composite(data_new, i,m1_f, sigmabrtf[i], sigmabrcf[i])
      plywise_value= {}
      total_damage={}
# storing the result of data for respective ply obtained from composite function
      plywise_value["Ply"+str(i+1)] = result_value[0]
      total=0
# Miner's sum of all damage for all R value obtained for each ply
      for number in result_value[1]:
          total+=number
      total_damage["Ply"+str(i+1)+"  fibre damage"] = total
# only to save damage value to find maximum
      collection_damage_fibre_value.append(total)
      plycollection_fibre.append(plywise_value)
      damage_collection_fibre.append(total_damage)
  return plycollection_fibre,damage_collection_fibre,collection_damage_fibre_value


# Function considering the work for matrix
def matrix(data_Y,data_XY,sigmabrtm,sigmabrcm,tau,dataset,n_laminate):
  f2=[]
  data_matrix=[]
  for i in range(len(data_Y)):
    data_Ymat = data_Y[i].T.squeeze()
    data_XYmat = data_XY[i].T.squeeze()
# loop to check the sigma_y value for all time step to evaluate the f2 value
    for j in range(len(data_Ymat)):
# ratio of normal stress to shear
        if data_Ymat[j]>=0:
            f=sigmabrtm[i]/tau[i]
        elif data_Ymat[j]<0:
            f=sigmabrcm[i]/tau[i]
        f2.append(f)
# evaluating the equivalent matrix stress
        datam=math.sqrt((data_Ymat[j])**2+(f2[j]*data_XYmat[j])**2)
        data_matrix.append(datam)
# define to store the matrix value plywise
  chunked_list = list()
  chunk_size = len(dataset)
  for i in range(0, len(data_matrix), chunk_size):
      chunked_list.append(data_matrix[i:i+chunk_size])

  plycollection_matrix=[]
  damage_collection_matrix=[]
  collection_damage_matrix_value=[]
  for i in range(0,n_laminate):
      data_new=pd.DataFrame(chunked_list[i]).T.squeeze()
# importing the commmon part of formula for matrix
      result_value = composite(data_new, i,m1_m, sigmabrtm[i], sigmabrcm[i])

      plywise_value = {}
      total_damage={}
      total=0
# Miner's sum of all damage fo all R value obtained for each ply
      for number in result_value[1]:
```

```
    total+=number
    total_damage["Ply"+str(i+1)+"  matrix_damage"] = total
# only to save damage value to find maximum
        collection_damage_matrix_value.append(total)
# storing the result of data for respective ply obtained from composite function
        plywise_value["Ply"+str(i+1)] = result_value[0]
        plycollection_matrix.append(plywise_value)
        damage_collection_matrix.append(total_damage)

    return plycollection_matrix,damage_collection_matrix,collection_damage_matrix_value


# defining the function for the common part
def composite(data_value,i,m_1,sigmabrt, sigmabrc):
    count=0
    data_new = data_value
    stresscollection=[]
    tempcollection=None
    damage_value=[]

# using rainflow algorithm
    for rng, mean, count, i_start, i_end in rainflow.extract_cycles(data_new):
        tempcollection=None
# stress range
        stressrange = rng
# mean stress
        stress_average_value = mean
# cycle count for given R
        cycles = count
# maximum stress for given R
        stress_maxR = (stressrange+2*stress_average_value)/2
# minimum stress for given R
        stress_minR = (2*stress_average_value-stressrange)/2
# alternating stress for given R
        alternate_stressR=stressrange/2
# stress ratio
        R = stress_minR / stress_maxR
# alternate stress ratio
        rho = (1 + R) / (1 - R)
# defining the area for different rho value using CFL diagram
        if rho > p1_value[1]:
            R_1 = R1[1]
            m1 =m_1[1]
            R_3 = 1
            m3 = 0
# Though value of m is mentioned here, it is not in use in any calculation. It is just for simplicity
        elif rho < p1_value[2]:
            R_1 = R1[2]
            m1 = m_1[2]
            R_3 = 1
            m3 = 0
        elif p1_value[0] < rho < p1_value[1]:
            R_1 = R1[1]
            m1 = m_1[1]
            R_3 = R1[0]
            m3 = m_1[0]
        elif p1_value[2] < rho < p1_value[0]:
            R_1 = R1[2]
```

```
        m1 = m_1[2]
        R_3 = R1[0]
        m3 = m_1[0]

    p_1 = (1 + R_1) / (1 - R_1)
    if R_3 == 1:
        p_3 = 0
    else:
        p_3 = (1 + R_3) / (1 - R_3)

    log_N1 = []
    N_1 = []
    sigmamax = []
    alternate_stress_value=[]
    stress_mean_value=[]


# evlauting all parameters for different stress_i value to plot SN curve
    for l in range(len(sigma_i1) - 1):
# formula for SN curve
        logN1 = -m1 * math.log10(sigma_i1[l] / 100)
        N1 = 10 ** logN1
# checking criteria for tensile or compression
        if sigmabrc / sigmabrt <= R_1 < 1:
# maximum stress for R_1
            sigma_max1 = sigma_i1[l] * sigmabrt / 100
# minimum stress for R_1
            sigma_min1 = sigma_max1 * R_1
        else:
            sigma_min1 = sigma_i1[l] * sigmabrc / 100
            sigma_max1 = sigma_min1 / R_1
        sigma_alt1 = (sigma_max1 - sigma_min1) / 2
        sigma_mean1 = (sigma_max1 + sigma_min1) / 2
# area at the axis
        if R_3==1:
            sigma_max3 = 0
            sigma_min3 = 0
            sigma_alt3 = 0
            sigma_mean3 = 0
# checking the tensile or compression region
            if sigmabrc / sigmabrt <= R_1 < 1:
# since only one R is avaliable, the formual used is of sigma_uts or sigma_ucs from Composite Guidelines from
BV
                sigma_alt = sigmabrt / (sigmabrt / sigma_alt1 + rho - p_1)
            else:
                sigma_alt = sigmabrc / (sigmabrc / sigma_alt1 + rho - p_1)
# maximum stress used for SN curve
            sigma_max = 2 * sigma_alt / (1 - R)
# minimum stress used for SN curve
            sigma_min = R * sigma_max
# mean stress used for SN curve
            sigma_mean = (sigma_max + sigma_min) / 2

# If interpolation is to be done within two different R values
        else:
            if sigmabrc / sigmabrt <= R_3 < 1:
                sigma_max3 = sigma_i1[l] * sigmabrt / 100
                sigma_min3 = sigma_max3 * R_3
```

```
            else:
                sigma_min3 = sigma_i1[l] * sigmabrc / 100
                sigma_max3 = sigma_min3 / R_3
            sigma_alt3 = (sigma_max3 - sigma_min3) / 2
            sigma_mean3 = (sigma_max3 + sigma_min3) / 2

# Formula used for interplation of maximum stress between two different R
            sigma_alt = sigma_alt1 * (p_1 - p_3) / ((p_1 - rho) * sigma_alt1 / sigma_alt3 + rho - p_3)
            sigma_mean = sigma_alt*rho
            sigma_max = sigma_mean + sigma_alt
            sigma_min = sigma_mean - sigma_alt
        log_N1.append(logN1)
        sigmamax.append(sigma_max)
        alternate_stress_value.append(sigma_alt)
        stress_mean_value.append(sigma_mean)

# Used for interpolation of logN and sigma max supplying data for SN curve
    y_f=interp1d(sigmamax,log_N1,fill_value="extrapolate")
# define the Number of cycle to damage for obtained maximum stress from rainflow for given R
    Number_of_cycle_to_damage = 10**y_f(stress_maxR)
    Number_of_cycle_to_fatigue=nb_cycle_fatigue*cycles
# evaluate damage
    damage=Number_of_cycle_to_fatigue/Number_of_cycle_to_damage
    damage_value.append(damage)

    tempcollection = {
        "R":R,
        "N":Number_of_cycle_to_damage,
        "logN":log_N1,
        "alternate stress":alternate_stress_value,
        "mean stress":stress_mean_value,
        "max stress":sigmamax,
        "maximum stress":stress_maxR
    }

    stresscollection.append(tempcollection)
  return stresscollection, damage_value


class CompositeCalculation():
  def run(self):
    return fibre( n_laminate,data_fibre,sigmabrtf,sigmabrcf),matrix(data_Y, data_XY,sigmabrtm,
sigmabrcm,tau,dataset,n_laminate)
# calculation result
if __name__ == '__main__':
  result = CompositeCalculation().run()
  fibre_result=result[0]
  matrix_result=result[1]
  fibre_damage_plywise=fibre_result[2]
  matrix_damage_plywise=matrix_result[2]
  location_maximum_damage_fibre=fibre_damage_plywise.index(max(fibre_damage_plywise))
  max_damage_fibre_location={}
  max_damage_fibre_location["Ply"+str(location_maximum_damage_fibre+1)] = max(fibre_result[2])
  location_maximum_damage_matrix=matrix_damage_plywise.index(max(matrix_damage_plywise))
  max_damage_matrix_location={}
  max_damage_matrix_location["Ply"+str(location_maximum_damage_matrix+1)] = max(matrix_result[2])
```